energy harbor

Energy Harbor Nuclear Corp.
Perry Nuclear Power Plant
10 Center Road
P.O. Box 97
Perry, Ohio 44081

Rod L. Penfield
Site Vice President, Perry Nuclear

440-280-5382

January 5, 2022
L-21-282

10 CFR 50.55a

ATTN: Document Control Desk
U.S. Nuclear Regulatory Commission
Washington, DC 20555-0001

Subject:
Perry Nuclear Power Plant
Docket No. 50-440, License No. NPF-58
Proposed Inservice Inspection Alternative IR-063

In accordance with 10 CFR 50.55a(z)(1), Energy Harbor Nuclear Corp. hereby requests Nuclear Regulatory Commission (NRC) staff approval of a proposed inservice inspection alternative to the American Society of Mechanical Engineers Section XI, Table IWB-2500-1, "Examination Category B-D, Full Penetration Welded Nozzles in Vessels," for use at Perry Nuclear Power Plant. The proposed alternative is enclosed and identifies the affected components, applicable code requirement, and a description and basis for the proposed alternative.

NRC staff review and approval of the proposed alternative is respectfully requested by January 31, 2023 to allow for application of the alternative during the spring 2023 refueling outage.

There are no regulatory commitments contained in this submittal. If there are any questions or if additional information is required, please contact Mr. Phil H. Lashley, Manager - Fleet Licensing, at (330) 696-7208.

Sincerely,

Rod L. Penfield

Enclosure: 10 CFR 50.55a Request IR-063

cc: NRC Region III Administrator
NRC Resident Inspector
NRC Project Manager

Enclosure
L-21-282

10 CFR 50.55a Request IR-063

(7 pages follow)

1. ASME Code Components Affected

Code Class: Class 1
Description: Reactor Pressure Vessel (RPV) Reactor Feedwater (RFW) Nozzles
Examination Category: B-D
Item Numbers: B3.90
B3.100
Component IDs:

Table 1

Component ID	Component Description	ASME Item No.
1B13-N4A-KA	Feedwater Nozzle N4A to Vessel	B3.90
1B13-N4A-IR	Feedwater Nozzle N4A Inner Radius	B3.100
1B13-N4B-KA	Feedwater Nozzle N4B to Vessel	B3.90
1B13-N4B-IR	Feedwater Nozzle N4B Inner Radius	B3.100
1B13-N4C-KA	Feedwater Nozzle N4C to Vessel	B3.90
1B13-N4C-IR	Feedwater Nozzle N4C Inner Radius	B3.100
1B13-N4D-KA	Feedwater Nozzle N4D to Vessel	B3.90
1B13-N4D-IR	Feedwater Nozzle N4D Inner Radius	B3.100
1B13-N4E-KA	Feedwater Nozzle N4E to Vessel	B3.90
1B13-N4E-IR	Feedwater Nozzle N4E Inner Radius	B3.100
1B13-N4F-KA	Feedwater Nozzle N4F to Vessel	B3.90
1B13-N4F-IR	Feedwater Nozzle N4F Inner Radius	B3.100

2. Applicable Code Edition and Addenda

American Society of Mechanical Engineers (ASME) Boiler and Pressure Vessel Code, Section XI, “Rules for Inservice Inspection of Nuclear Power Plant Components,” 2013 Edition (no Addenda).

3. Applicable Code Requirement

The applicable Code requirement is contained in ASME Section XI, Division 1, Subsection IWB, Table IWB-2500-1, “Examination Category B-D, Full Penetration Welded Nozzles in Vessels.” Class 1 nozzle-to-vessel welds and nozzle inner radii examination requirements are delineated in Item Numbers B3.90, “Nozzle-to-Vessel Welds,” and B3.100, “Nozzle Inside Radius Section.” The method of

examination is volumetric. With respect to the extent of examination, all nozzles with full penetration welds to the vessel shell (or head) and integrally cast nozzles must be examined each interval.

4. Reason for Request

The proposed alternative provides an acceptable level of quality and safety based on a plant-specific evaluation using a probability fracture mechanics (PFM) methodology endorsed by the Nuclear Regulatory Commission (NRC) in Electrical Power Research Institute (EPRI) Technical Reports BWRVIP-108-A, "Technical Basis for the Reduction of Inspection Requirements for the Boiling Water Reactor Nozzle-to-Vessel Shell Welds and Nozzle Inner Radii," [Reference 1] and BWRVIP-241-A, "Probabilistic Fracture Mechanics Evaluation for the Boiling Water Reactor Nozzle-to-Vessel Shell Welds and Nozzle Blend Radii," [Reference 2].

5. Proposed Alternative and Basis for Use

In lieu of performing examinations on 100 percent of the population of RFW nozzle assemblies, Energy Harbor Nuclear Corp. proposes to examine a minimum of 25 percent of the population of the nozzle-to-vessel welds and a minimum of 25 percent of the population of the inner radii using volumetric inspection methods performed in accordance with ASME Section XI, Appendix VIII, "Performance Demonstration for Ultrasonic Examination Systems," as modified by 10 CFR 50.55a.

Basis for Use

EPRI Technical Reports BWRVIP-108-A [Reference 1] and BWRVIP-241-A [Reference 2] contain the technical basis supporting ASME Boiler and Pressure Vessel Code Case N-702, "Alternative Requirements for Boiling Water Reactor Nozzle Inner Radius and Nozzle-to-Shell Welds, Section XI, Division 1" [Reference 3] for reducing the inspection of RPV nozzle-to-vessel welds and nozzle inner radius regions from 100 percent of the population of the nozzles to 25 percent of the population of nozzles for each nozzle type during each 10-year ISI interval. However, the reports and Code Case N-702 explicitly exclude reactor feedwater nozzles stating that these nozzles are managed under a separate mandated program directed by NUREG-0619, "BWR Feedwater Nozzle and Control Rod Drive Return Line Nozzle Cracking: Resolution of Generic Technical Activity A-10 (Technical Report)" [Reference 4]. This request proposes that the RFW nozzle-to-vessel welds and inner radii examinations mandated under NUREG-0619 can be subsumed by the current ASME Section XI requirements and the number of inspections reduced based on this relief request.

Discussion on NUREG-0619

The Perry Nuclear Power Plant (Perry) complies with the inspection requirements of NUREG-0619 by implementation of the NRC approved alternative

GE-NE-523-A71-0594-A, [Reference 5], which stipulates inspections for the RFW nozzle inner radii, nozzle inner bore regions, and the spargers. The nozzle inner radii inspections are performed in compliance with ASME Section XI, as modified by the Performance Demonstrated Initiative (PDI) Program description and meets the established criteria of Reference 5. Section 6.3 of Reference 5 states that after compliance with ASME Section XI, Appendix VIII, the examination frequency will be the ASME Section XI examination frequency for non-interference fit plants such as Perry.

NUREG-2221, "Technical Bases for Changes in the Subsequent License Renewal Documents NUREG-2191 and NUREG-2192," December 2017, states that the recommendation for condition monitoring of the RFW nozzles be performed under ASME Section XI ISI inspections for the condition monitoring basis for managing cracking in boiling water reactor (BWR) feedwater nozzles induced by cyclical loading mechanism. This is based in part on improvements in ASME Section XI directed volumetric examination techniques, which now meet the requirements proposed in Reference 5. Thus, there is a general acknowledgement that the RFW nozzle examinations need no longer go beyond ASME Section XI guidelines and a separate mandated program is not required.

Justification for Reduction to 25 Percent

One of the criteria for demonstrating plant-specific applicability of BWRVIP-108-A [Reference 1] and BWRVIP-241-A [Reference 2] is to show that the maximum RPV heatup and cooldown rate for the unit is limited to less than 115°F per hour. Perry Technical Specification 3.4.11, "RCS Pressure and Temperature (P/T) Limits," limits the maximum reactor vessel operational heatup and cooldown rates to less than or equal to 100°F per hour, which is within the 115°F per hour limit. Therefore, this criterion is satisfied.

Using the same analytical methodology as employed in BWRVIP-108-A and BWRVIP-241-A [References 1 and 2], it can be shown that Perry's RFW nozzle failure probabilities due to a low temperature over pressure (LTOP) event at the nozzle radius region and the nozzle-to-vessel weld are very low and meet the NRC acceptance criteria in NUREG-1806, "Technical Basis for Revision of Pressurized Thermal Shock (PTS) Screen Limit in the PTS Rule (10 CFR 50.61)." Based on the results of the plant-specific evaluation, and industry and internal operating experience, the inspection of 25 percent of the population of RFW nozzles is considered technically justified.

The plant-specific PFM analysis employed a Monte Carlo simulation using Structural Integrity Associates, Inc. proprietary software VIPERNOZ, which was developed for RPV nozzle weld inspection with BWRVIP-108-A. Perry's nozzle stresses are used with probabilistic distributions from BWRVIP-108-A and BWRVIP-241-A [References 1 and 2] to evaluate the plant specific probabilities. Stress results for Perry are provided in Attachment 1 of this request. The PFM evaluation is provided in

Attachment 2. The attached plant-specific analysis conservatively extends to 60 years. The PFM evaluation conclusions are summarized in Section 5.0 of Attachment 2.

For normal operation, the results for Stress Path 1 at the nozzle blend radius bounds the other stress paths. For Stress Path 1, five (5) failures occurred during normal operation in 1 million simulations for 60 years of plant operation. The probability of failure (PoF) for normal operation for Stress Path 1 is calculated to be 5 failures / 1 million simulations / 60 years = 8.33×10^{-8} per year. The calculated PoF for normal operation for Stress Path 1 is less than the allowable PoF of 5.0×10^{-6} per year from NUREG-1806.

For LTOP events, the results for Stress Path 1 at the nozzle blend radius bounds the other stress paths. For Stress Path 1, 52 LTOP failures occurred in 1 million simulations for 60 years of plant operation. The conditional PoF for LTOP events for Stress Path 1 is calculated to be 52 failures / 1 million simulations / 60 years = 8.67×10^{-7} per year. Accounting for an LTOP event occurrence of 1.0×10^{-3} per year, the calculated PoF for LTOP events for Stress Path 1 is 8.67×10^{-10} per year, which is less than the allowable PoF of 5.0×10^{-6} per year from NUREG-1806.

The PFM results are also confirmed by a deterministic fracture mechanics (DFM) evaluation (Attachment 2, Appendix A), using the methodology in Section 6 of BWRVIP-108-A.

Thus, using the PFM methodology in BWRVIP-108-A and BWRVIP-241-A, which is the technical basis for ASME Code Case N-702, the Perry feedwater nozzles are qualified for inspection relief from 100 percent to 25 percent of the feedwater nozzle population every 10 years from the fourth 10-year ISI interval for up to 60 years of plant operation.

Code Case N-702 is listed in Regulatory Guide (RG) 1.147, Revision 19, Table 2, “Conditionally Acceptable Section XI Code Cases.” The required condition associated with Code Case N-702 is as follows:

> The applicability of Code Case N-702 for the first 40 years of operation must be demonstrated by satisfying the criteria in Section 5.0 of NRC Safety Evaluation regarding BWRVIP-108 dated December 18, 2007 (ML073600374) or Section 5.0 of NRC Safety Evaluation regarding BWRVIP-241 dated April 19, 2013 (ML13071A240).

The condition is intended to verify the applicability of the technical basis documents [References 1 and 2] to the licensee’s design. Because the technical basis documents exclude the RFW nozzles, the Code Case is not applicable; however, Energy Harbor Nuclear Corp. considers the intent of the Code Case, the condition, and acceptance criteria are demonstrated by the plant-specific analysis for Perry.

Perry Operating Experience

A detailed evaluation of the historical problems of the RFW nozzle and sparger is presented in NEDE-21821, "BWR Feedwater Nozzle / Sparger Final Report," March 1978. The solution of the feedwater nozzle and sparger cracking problems involved several elements, including material selection and processing, nozzle clad elimination, and thermal sleeve and sparger redesign. Perry implemented these changes during construction including clad elimination around the nozzle and a welded thermal sleeve and safe end design.

As documented in Perry's Updated Safety Analysis Report Section 5.3.3.3, "The shell and vessel head were made from formed low alloy steel plates, and the flanges and nozzles from low alloy steel forgings." The section goes on to state, "Post weld heat treatment of 1,100°F minimum was applied to all low alloy steel welds." This heat treatment should reduce residual stresses from any repairs such that they would not be a dominant force requiring consideration in the analysis. Weld residual stress (after post weld heat treatment) was included in the probabilistic fracture mechanics design input as described in Attachment 2.

A review of the most recent examination results for each component listed in Table 1 identified all ultrasonic examination results were acceptable to the requirements of ASME Boiler and Pressure Vessel Code Section XI, 2001 Edition with the 2003 Addenda. All of the examinations were volumetric, using ultrasonic testing (UT) methodology performed in accordance with ASME Section XI, 2001 Edition and 2003 Addenda, and as modified by the PDI program and 10 CFR 50.55a requirements. All of the inner radius welds in Table 1 had 100 percent exam coverage. All of the nozzle-to-vessel welds had greater than or equal to 82.7 percent exam coverage. Table 2 describes the coverage, exam method, and when the most recent exam occurred for each weld. The reduced exam coverage for the nozzle-to-vessel welds was due to nozzle forging configurations, for which relief was granted in the NRC safety evaluation dated September 18, 2020 (Accession No. ML20252A026). Only the volumetric examinations required by ASME Section XI, Table IWB-2500-1 Category B-D are discussed in this request.

Table 2				
Component ID	**Description**	**Year of Last Exam Performed**	**Exam Method**	**Percent Coverage**
1B13-N4A-KA	Feedwater Nozzle N4A to Vessel	2013	UT	83.2%
1B13-N4A-IR	Feedwater Nozzle N4A Inner Radius	2013	UT	100%
1B13-N4B-KA	Feedwater Nozzle N4B to Vessel	2013	UT	83.2%
1B13-N4B-IR	Feedwater Nozzle N4B Inner Radius	2013	UT	100%
1B13-N4C-KA	Feedwater Nozzle N4C to Vessel	2013	UT	83.2%
1B13-N4C-IR	Feedwater Nozzle N4C Inner Radius	2013	UT	100%
1B13-N4D-KA	Feedwater Nozzle N4D to Vessel	2013	UT	83.2%
1B13-N4D-IR	Feedwater Nozzle N4D Inner Radius	2013	UT	100%
1B13-N4E-KA	Feedwater Nozzle N4E to Vessel	2013	UT	82.7%
1B13-N4E-IR	Feedwater Nozzle N4E Inner Radius	2013	UT	100%
1B13-N4F-KA	Feedwater Nozzle N4F to Vessel	2013	UT	83.2%
1B13-N4F-IR	Feedwater Nozzle N4F Inner Radius	2013	UT	100%

Industry Operating Experience

NUREG-0619 was published in November 1980 to address instances of thermal fatigue cracking of the RFW and control rod drive return line nozzle. The guidance gave design, operating, and inspection recommendations to address these concerns. As identified in a July 25, 2006 BWRVIP letter to the NRC (Accession No. ML062080159), a survey of all U.S. BWRs shows the majority of RPV nozzles had no reportable indications in the nozzle-to-vessel weld or their inner radii. A few nozzles contained subsurface indications, which were determined to be acceptable. The data in the letter indicates that the inspections performed as of that date, using reliable techniques, have shown that there are no active degradation mechanisms for the nozzle-to-vessel welds and inner radii regions. A search of the Institute of Nuclear Power Operations (INPO) database performed in December of 2021 found that this trend appears to continue with no reports of indications in RPV nozzle-to-vessel welds or inner radii regions found.

Proposed Alternative

Energy Harbor Nuclear Corp. proposes to inspect 25 percent of the population of RFW nozzle-to-vessel welds and inner radius regions each 10-year ISI inspection interval at Perry using volumetric inspection methods that meet or exceed the requirements of ASME Section XI, 2013 Edition (no addenda), Appendix VIII, “Performance Demonstration for Ultrasonic Examination Systems,” as modified by 10 CFR 50.55a. The plant-specific evaluation performed for Perry’s RFW nozzles shows that for a 60-year plant life, the failure probabilities due to a LTOP event at the nozzle inner radius region and the nozzle-to-vessel weld meet the acceptance criterion in NUREG-1806. Hence, the alternative provides an acceptable level of quality and safety pursuant to 10 CFR 50.55a(z)(1) for the RFW nozzle-to-vessel welds and nozzle inner radii sections identified in Table 1.

This proposed alternative does not seek relief from any other aspect of the ASME Section XI Code. Therefore, if an indication is detected that exceeds ASME inspection criteria, scope expansion (extent of condition) will still be performed in accordance with ASME Section XI, subsection IWB-2430, “Additional Examinations,” for the Code of Record in place at the time of discovery.

6. Duration of Proposed Alternative

The proposed alternative is requested for the remainder of the fourth 10-year ISI inspection interval that ends on May 17, 2029, recognizing that the existing 40-year license expires November 7, 2026.

7. Precedent

Relief to inspect 25 percent of the RFW nozzle-to-vessel welds and inner radius regions each 10-year ISI interval was authorized for Columbia Generating Station, Docket No. 50-397, by NRC safety evaluation dated April 14, 2021 (ADAMS Accession No. ML21096A048). The relief was approved for the remainder of the 60-year plant life, including the period of extended operation.

8. References

1. BWRVIP-108-A, “Technical Basis for the Reduction of Inspection Requirements for the Boiling Water Reactor Nozzle-to-Vessel Shell Welds and Nozzle Blend Radii, EPRI, Palo Alto, CA: 2018, 3002013092.

2. BWRVIP-241-A, “Probabilistic Fracture Mechanics Evaluation for the Boiling Water Reactor Nozzle-to-Vessel Shell Welds and Nozzle Blend Radii,” EPRI, Palo Alto, CA: 2018, 3002013093.

3. ASME Boiler and Pressure Vessel Code, Code Case N-702, “Alternative Requirements for Boiling Water Reactor (BWR) Nozzle Inner Radius and Nozzle-to-Shell Welds, Section XI, Division 1,” February 20, 2004.

4. NUREG-0619, “BWR Feedwater Nozzle and Control Rod Drive Return Line Nozzle Cracking: Resolution of Generic Technical Activity A-10 (Technical Report),” Revision 1, November 1980.

5. GE-NE-523-A71-0594-A, “Alternate BWR Feedwater Nozzle Inspection Requirements,” Revision 1, May 2000

Attachment 1
10 CFR 50.55a Request IR-063

Feedwater Nozzle Loads, Finite Element Model, and Stress Analysis

(44 pages follow)

File No.: 2001178.301
Project No.: 2001178
Quality Program Type: ☒ Nuclear ☐ Commercial

CALCULATION PACKAGE

PROJECT NAME:
Perry Feedwater Nozzle PFM Evaluation and Inspection Relief Request

CONTRACT NO.:
48309846

CLIENT:
Energy Harbor

PLANT:
Perry Nuclear Power Plant

CALCULATION TITLE:
Feedwater Nozzle Loads, Finite Element Model, and Stress Analysis

Document Revision	Affected Pages	Revision Description	Project Manager Approval Signature & Date	Preparer(s) & Checker(s) Signatures & Date
0	1 - 28 A-1 - A-2 B-1 - B-13	Reissue with typographical changes in red for Table 3 by Kevin Wong (KLW) 12/22/21	Kevin Wong 12/17/21	Garivalde S. Dominguez 12/17/21 Kevin Wong 12/17/21 Charles Fourcade 12/17/21

Table of Contents

List of Tables

List of Figures

1.0 OBJECTIVE

The objective of this calculation is to establish the design inputs and methodology, modify a previously developed finite element model (FEM) and perform stress analysis to be used in the probabilistic fracture mechanics (PFM) evaluation of reactor pressure vessel (RPV) feedwater (FW) nozzle at Perry Nuclear Power Plant (Perry).

2.0 METHODOLOGY

Stress distributions due to pressure, thermal transient, and mechanical loads will be used in the subsequent PFM evaluation. A three step methodology is performed herein:

i. Loads: Establish design inputs and methodology to be used in the FEM. A thermal transient analysis will be performed based on system thermal cycling that occurs at the FW nozzle. Concurrent with the thermal transients, pressure and piping interface loads are also considered. Power uprate affects the FW temperature and rated flow per nozzle as shown in Table 1 [1].

ii. FEM: Modify a previously developed three-dimensional (3-D) finite element model (FEM) of the Perry feedwater nozzle [2] to be used in the stress analyses. Additional methodology for the FEM development was established in a previous loads calculation [3] and are noted herein.

iii. Stress Analyses: Perform stress evaluation by applying loads to the FEM and obtain stress distributions for the RPV FW nozzle at the nozzle blend radius and nozzle-to-shell weld.

3.0 ASSUMPTIONS

All assumptions except Assumption 5 (i.e., the assumption regarding the RPV cladding) associated with the previous FEM calculation [2 , Section 2.0] are applicable to this calculation. All assumptions associated with the previous loads calculation [3, Section 3.0] are applicable to this calculation.

The following are additional assumptions within this calculation:

a. For Transient 4b (Turbine Roll), 4140 seconds is calculated by assuming a decrease rate of 100°F/hr.
b. For Transient 22 (Reactor Overpressure), a conservative approach is assumed by omitting the steady-state temperature after 2760 seconds with “indefinite time” in the transient.

4.0 DESIGN INPUTS AND LOADS

4.1 Thermal Transients

The thermal cycle diagrams for the FW nozzle [6] and RPV [7] were used to define the thermal transients in Table 3; in addition, power uprate conditions [1] in Table 1 are applied.

Table 2 lists the projected 60-year cycles [4.a, Tables 8 & 9] with the following notes:

- For the following transients, the 60-year projected cycles are a summation of the normal and alternate transients:
    - Transient 3 (Startup): Normal Startup 3-A and Alternate Startup 3-B.

- Transient 4 (Turbine Roll): Normal Turbine Roll 4-A and Alternate Turbine Roll 4-B.
- Transient 14 (Hot Standby): Normal Shutdown - Hot Standby 14-A and Alternate Shutdown - Hot Standby 14-B.
- Transient 15 (Shutdown): Normal Shutdown – Blowdown to Condenser 15-A and Alternate Shutdown - Blowdown to Condenser 15-B.
- For Transient 16 (Shutdown, Vessel Flooding): Normal Shutdown – Vessel Flood 16-A and Alternate Shutdown – Vessel Flood 16-B.

- It is assumed that there are 40 internal cycles for each OBE event [4.b]. Therefore, 2 OBE events × 40 internal cycles = 80 OBE cycles are evaluated for 60 years of plant operation.

4.2 Bounding Transients

The transients are then screened to obtain the limiting events that bound the other transients. The limiting events are shaded in grey in Table 3. The criteria for selecting the worst cases are (a) transients that have a large temperature difference and (b) transients that have a drastic rate of change in temperature. The screening method is calculated in the supporting spreadsheet *2001178.301-FW_Bounding_Transient_Screening.xlsm,* and the following transients are selected as bounding:

(1) Transient 3b (Start-up): For the FW temperature side (T_{FW}), the event has a step-down temperature change from 400°F to 185°F (see Table 3). For the RPV temperature side (T_A): the event has temperature range from 100°F to 552°F, with temperature rate of change of 100°F/hr.

(2) Transient 4b (Turbine Roll): For the T_{FW} side, the event has a temperature change from 70°F to 325°F in 2 minutes duration (see Table 3).

(3) Transient 6 (Daily Reduction, 50% Power): This transient is included to segregate the high cycle yet less severe events such as “Daily reduction to 50% power” and “Rod pattern change” from the other thermal transients that generates high stresses.

(4) Transient 8 (Turbine Trip): For the T_{FW} side, the event has a temperature change from 427.8°F to 90°F in 1.5 minutes duration (see Table 3).

(5) Transient 10 (Turbine Generator Trip): For the T_{FW} side, the event has a of temperature change from 427.8°F to 275°F in 1 minute duration. For the T_A side, the event has temperature change from 552°F to 350°F both in increasing and decreasing direction (see Table 3).

(6) Transient 15b (Shutdown): For the T_{FW} side, the event has a step-down temperature change from 425°F to 200°F (see Table 3). For the T_A side, the event has temperature range from 502°F to 250°F, with temperature rate of change of 100°F/hr.

(7) Transient 20 (Loss of FW pumps): For the T_{FW} side, the event has a step-down temperature change from 485°F to 100°F (see Table 3). For the T_A side, the event has temperature range from 350°F to 582°F.

(8) Transient 21 (Safety Relief Valve (SRV) Blow Down): For the T_{FW} side, the event has a step-down temperature change from 427.8°F to 275°F and from 275°F to 100°F (see Table 3). For the T_A side, the event has temperature range from 552°F to 375°F in 10 minutes duration.

(9) Transient 22 (Reactor Overpressure): For the T_{FW} side, the event has a step-down temperature change from 427.8°F to 275°F (in 1 minute) and from 275°F to 100°F (in 15 minutes) (see Table 3). For the T_A side, the event has temperature range from 561°F to 400°F in 15 minutes duration.

4.3 Mechanical Loads

The mechanical loads [5] are shown in Table 4. Mechanical forces and moments are listed in kips and inch-kips, respectively. The thermal sleeve mechanical loadings [5] are small and are considered to be negligible; thus the thermal sleeve mechanical loadings shall not be evaluated.

5.0 FINITE ELEMENT MODEL

The details of the previously developed FEM are provided in the previous FEM [2] and loads [3] calculations:

- Geometry: Figure 1 shows the dimensions of the FEM based on nozzle drawings referenced in the previous FEM calculation [2, Section 3.1] with additional modifications described in the subsequent sections.

- Materials: Figure 2 shows the materials used in the FEM, and the material properties are tabulated in the previous FEM calculation [2, Table 1]. The material and material properties of the added cladding are described in the next section.

- Applied Fluid Temperatures: The calculation of applied fluid temperatures follows the methodology in the previous loads calculation [3, Section 4.5] for the thermal transients in Table 3. Detailed calculations of the applied fluid temperatures are provided in Appendix B and documented in the supporting files.

- Heat Transfer Coefficients: The calculation of heat transfer coefficients by forced convection, natural convection, and steam condensation as a function of feedwater flow and location follows the methodology in the previous loads calculation [3, Sections 4.6 and 4.7]. Detailed calculations of the heat transfer coefficients are provided in Appendix B and documented in the supporting files.

- Assumptions: All assumptions except Assumption 5 (i.e., the assumption regarding the RPV cladding) associated with the previous FEM calculation [2 , Section 2.0] are applicable to this calculation. All assumptions associated with the previous loads calculation [3, Section 3.0] are applicable to this calculation.

The FEM is a quarter model which consists of two axes of symmetry in the longitudinal and circumferential directions of the vessel shell (Figure 5). Hence, a quarter model (0° to 90°) with the appropriate boundary conditions is adequate for the stress analysis of loads that were axisymmetric and resulted in the same stresses as a 360° model. For mechanical piping load which are not axisymmetric, a separate full 3-D FEM (360° model) is constructed from the quarter size model by reflecting about the symmetry planes (Figure 10). Piping interface moments were applied at one free end of the pipe.

Two minor modifications described in the subsequent sections are made to the previously developed FEM for this stress analysis. The modified FEM is documented in the supporting files in Appendix A.

5.1 RPV Cladding

The previously developed FEM did not model the RPV cladding [3 , Section 2.0, Assumption 5], since the location of interest for the previous analysis was sufficiently far away from the clad regions. For this stress analysis and the subsequent PFM evaluation of the nozzle blend radius and the nozzle-to-shell weld, the RPV cladding of a nominal thickness of 3/16 inch [8, Sheet 1 of 23] has been added to the FEM at the RPV inner surface, as shown in Figure 2. The modeling of the nominal thickness is

conservative with regards to stresses compared to the minimum specified thickness. The RPV cladding is modeled as 309/308L Austenitic Stainless Steel with material properties consistent with the Reference [2, Table 1]

5.2 Removal of Weld Overlay

One Perry feedwater nozzle has a weld overlay (WOL) [9] applied at the nozzle-to-safe end weld N4C-KB. The other Perry feedwater nozzles had a mechanical stress improvement process (MSIP) applied at the nozzle-to-safe end weld [10]. The stress effects of the WOL and MSIP are localized to the nozzle-to-safe end weld and the adjacent base metal. The region of interest at the nozzle blend radius and nozzle-to-shell weld for this evaluation is sufficiently far away (i.e., greater than one nozzle diameter) from the nozzle-to-safe end weld such that the effects of the WOL or MSIP at the region of interest are negligible, based on previous WOL stress evaluations. As such, the stresses at the region of interest are essentially the same for all the Perry feedwater nozzles irrespective of the WOL or MSIP.

The previously developed FEM included the WOL at the nozzle-to-safe end weld. Since the effects of the WOL are negligible at the nozzle blend radius and the nozzle-to-shell weld, the WOL has been removed from the FEM.

5.3 Mesh

A 3-D linear-elastic FEM of the FW nozzle is built using the finite element software ANSYS 14.5 [11]. The FEM consists of eight node SOLID45 structural elements (see Figure 3). These are converted to eight node SOLID70 thermal elements for thermal analyses. The ANSYS input files *FWgeom.INP* and *FWgeom-2.INP* can be read into ANSYS to create the FEM. ANSYS 14.5 [11] was used from Reference [2] and the same version was used to modify the FEM. For the stress analysis such as pressure stress analysis (see Section 5.4) and thermal transient and mechanical piping stress analysis (see Section 6.2 and 6.3), ANSYS 18.1 [12] is used.

5.4 Mesh Sensitivity Study

In order to verify that the mesh density of the FEM is adequate to capture stresses at the blend radius and safe end, a mesh sensitivity study is performed. A unit pressure analysis is performed by applying a 1000 psi pressure to the inside surfaces of the vessel and nozzle. Cap loads are applied to the top of the vessel and attached pipe end using the equation:

$$P_{cap} = \frac{P \cdot R_i^2}{R_o^2 - R_i^2} \tag{1}$$

where R_i is the inner radius of the vessel or attached piping and R_o is the outer radius of the vessel or attached piping.

These cap loads are given a negative sign in order to exert tension on the model. Nodes are also coupled in the axial direction for both the top of the vessel and the pipe section to simulate the attached vessel and piping, respectively. Symmetry boundary conditions are applied to the vertical and horizontal “cut planes” to simulate parts of the vessel that are not modeled. Figure 4 shows the pressure load applied to the FEM and Figure 5 shows the boundary conditions applied to the FEM. The ANSYS input file *Pressure.INP* contains the loading and boundary conditions for the pressure loading.

Figure 6 shows the mesh and pressure stress results at the blend radius for the original FEM. The original FEM has a maximum stress intensity of 50,097 psi. Figure 7 shows the mesh and pressure

stress results at the blend radius for the refined FEM. The refined FEM has a maximum stress intensity of 50,513 psi.

Since the stress intensity differences for nodes at the blend radius is less than 1% for the original and refined FEMs, the original mesh (as shown in Figure 3) is sufficient for future analyses.

The refined FEM ANSYS input files are saved in the supporting files as *FWgeom-Refined.INP* and *Pressure-Refined.INP* (see Appendix A)

6.0 STRESS ANALYSIS

The developed finite element model (FEM) of the Feedwater nozzle is used to perform thermal, pressure and mechanical piping stress analyses using the ANSYS FEA software [12]. A thermal analysis is performed for each transient defined in Section 4.2. Unit pressure and piping interface load analyses are performed separately from the thermal transient analyses. The details of the evaluations are discussed below.

6.1 Unit Pressure Stress Analysis

A 1000 psi unit pressure stress analysis is performed in Section 5.4.

6.2 Thermal Transient Stress Analysis

The FEM developed in Section 5.0 is used as input for the thermal transient stress analysis using ANSYS [12]. ANSYS SOLID45 structural elements are switched to SOLID70 thermal elements for thermal temperature distribution analysis. For thermal stress analysis, SOLID45 structural elements are used. The boundary conditions used for the thermal stress analysis are the same as those used for the pressure stress analysis, described in Section 5.4 and shown in Figure 5.

Previously defined bounding thermal transients in Section 4.2 are evaluated, applying heat transfer coefficients and fluid temperatures which are shown in Figure 8.

All ANSYS input files used for the thermal transient stress analysis, as listed below, are saved in the project computer files:

HTBC.INP:	Thermal boundary regions and heat transfer application
FWnoz_T#.INP: *FWnoz_T#_mntr.INP:* *FWnoz_S#.INP*:	Thermal and stress analysis input files Where "#" indicates the transient number

Transient Definitions:
- Transient 3b: Startup
- Transient 4b: Turbine Roll
- Transient 6: Weekly Reduction, 50% Power
- Transient 8: Turbine Trip
- Transient 10: Turbine Generator Trip
- Transient 15b: Shutdown
- Transient 20: Loss of FW Pump
- Transient 21: SRV Blowdown
- Transient 22: Reactor Overpressure

6.3 Piping Interface Loads Stress Analysis

For the attached piping interface loads stress analysis, a full 3-D FEM is used rather than the ¼ model used for the other analyses. The original geometry is modified to represent the full 3-D model. Mechanical piping interface loads are applied to the piping face of the FEM. The mechanical loading is outlined in Table 4. Deadweight, seismic primary, seismic restrained free end and thermal restrained free end loads are applied. Design mechanical loads are for primary stress checks and are not considered for fatigue. Since seismic primary and seismic restrained free loads are identical, a single seismic load case is analyzed. The ANSYS input file *FWnoz_Mechanical.inp* contains the seismic and thermal piping loads and boundary conditions for the piping stress analysis respectively.

Figure 9 shows the local coordinate system for the design forces and moments. These coordinates are modified to account for global ANSYS coordinates for use with the FEM. In order to account for the difference in applied location, "M" is corrected for by the equation:

$$M_{L,applied} = M_L + H \cdot L$$

where,	M_L	=	Applied moment, Figure 9
	H	=	Applied force, Figure 9
	L	=	Length from design location "R" (see Figure 9) to applied location
		=	(162.8025-151) = 11.8025 inch

where 162.8025 inches is obtained from the finite element model: from the center of the RPV to the FW piping end and 151 inch is obtained from Reference [5, Sheet 5].

Loads are applied using the ANSYS TARGE170 target element type to create a pilot node at the free end of the nozzle. The ANSYS CONTA175 contact element type is used to create a contact surface at the free end of the nozzle. The pilot node and surface are bonded together, so that the moment applied to the pilot node is transferred to the nozzle free end.

6.4 Critical Stress Paths

The critical stress paths are selected for two locations on the feedwater nozzle. Two paths (P1 and P2) are chosen at the blend radius, and two paths (P3 and P4) are chosen at the nozzle-to-shell weld. Detailed nodal location of paths are as follows:

- Path 1, P1: nozzle-to-vessel shell blend radius, x-z plane, from node 113476 to node 114562
- Path 2, P2: nozzle-to-vessel shell blend radius, y-z plane, from node 113521 to node 115123
- Path 3, P3: nozzle-to-vessel shell weld, x-z plane, from node 131478 to node 135428
- Path 4, P4: nozzle-to-vessel shell weld, y-z plane, from node 131469 to node 135395

The stress extraction is generated under RSYS = 0, where Path 1 and 3 results have the hoop stress in Y-direction and Path 2 and 4 results have the hoop stress X-direction.

7.0 CONCLUSION

The FW nozzle finite element model is developed, and pressure, thermal transients, and mechanical piping loads are applied to perform stress analyses. The stress results for each of the defined stress paths will be used in the subsequent PFM evaluation.

8.0 REFERENCES

1. GE Design Specification No. 26A5308, Revision 3, *Reactor Vessel – Power Uprate*, SI File No. 2001178.206.
2. SI Calculation No. 1300310.304, Revision 0, "Perry Feedwater Nozzle Finite Element Model."
3. SI Calculation No. 1300310.305, Revision 0, "Feedwater Nozzle Design Loads Calculation for use in Environmental Fatigue Analysis."
4. Projected 60-Year Cycles
   a. Structural Integrity Associates Calculation No. 2001140.301, Revision 1, "Fatigue Update for Perry Nuclear Power Plant from 10/1/2016 to 10/31/2021."
   b. Email from J. Zbiegien (Energy Harbor) to K. Wong (SI), "Subject: RE: [EXTERNAL] RE: Projected Cycles," December 3, 2021, 7:44AM, SI File No. 2001178.207.
5. GE Design Specification Data Sheet No. 22A5536AF, Revision 1, Safe End, Feedwater Nozzle, SI File No. 0800184.202.
6. Feedwater Thermal Cycle Diagrams
   a. Energy Harbor Drawing No. 306-0081-00000, Revision E, "Feedwater Temperature/Pressure Cycles," SI File No. 2001178.204.
   b. Energy Harbor Drawing No. 306-0082-00000, Revision D, "Feedwater Temperature/Pressure Cycles," SI File No. 2001178.204.
7. Reactor Thermal Cycle Diagrams
   a. Energy Harbor Drawing No. 08-0037-00001 (General Electric Drawing No. 762E458, Revision 7, Sheet 1, "Reactor Cycles"), SI File No. 20001178.203.
   b. Energy Harbor Drawing No. 08-0037-00002 (General Electric Drawing No. 762E458, Revision 7, Sheet 2, "Reactor Cycles"), SI File No. 2001178.203.
   c. Energy Harbor Drawing Update Notice No. 08-0596-001-001, Revision 0, "Reactor Cycles," SI File No. 2001178.203.
   d. Energy Harbor Drawing Update Notice No. 08-0596-001-003, Revision 0, "Reactor Cycles," SI File No. 2001178.203.
8. CBI Nuclear Company Section No. 238-D11.3, Revision 5, "Perry 1 – 238 BWR 6 Vessel Contract 73-C108, Stress Report (Code), Water Lev. Instr. Nozzle Design Report – Section D 11.3," SI File No. 2001178.212.
9. Energy Harbor IDCN No. 305-006-108-995013, Revision 1, "RV. Feedwater Nozzle Weld Arrangement," SI File No. 2001178.211.
10. Energy Harbor Calculation No. EA-0264, Revision 1, "Flaw Evaluation, Feedwater Nozzle B13-N4E-KB," SI File No. 2001178.210.
11. ANSYS Mechanical APDL and PrepPost, Release 14.5 (w/Service Pack 1), September 2012.
12. ANSYS Mechanical APDL (UP20170403) and Workbench (March 31, 2017), Release 18.1, SAP IP, Inc.

Table 1: Pre- and Post-Power Uprate Temperatures and Flow Rate

Parameter	Pre-Power Uprate	Post Power Uprate
100% Rated FW Flow/Nozzle (gpm)	7410* [1, sheet 35 of T4]	6555 [1]
FW Temperature (°F)	420 [1]	427.8 [1]

Note: * This is the as-analyzed flow rate; the actual flow rate before power uprate was lower than the power uprate value of 6555 gpm.

Table 2: Thermal Transient Definitions

Event	Description	60-Year Projected Cycles [4.a, Tables 8 & 9]
1	Boltup	37
2	Design hydrotest	47
3	Startup	166 + 10 (Note 1)
4	Turbine roll	167 +1 (Note 1)
5	Daily reduction	685
6	Weekly reduction	436
7	Rod pattern change	685
8	Turbine trip	22
9	Partial feedwater heater bypass	159
10	Turbine generator trip	13
11	Other scrams	87
13	Reduction to 0% power	209
14	Hot standby	127 + 4 (Note 1)
15	Shutdown	165 + 4 (Note 1)
16	Shut down, vessel flooding	160 + 10 (Note 1)
17	Shutdown	183
18	Unbolt	36
19	Refueling	33
20	Composite Loss of Feedwater	20
21	SRV blowdown	2
22	Reactor Overpressure	1
23	Automatic Blowdown	1
24	Improper Start of Cold Recirc Loop	1
25	Sudden Start of Pump in Cold Recirc Loop	4
27	Pipe Rupture	1
-	OBE	2 x 40 (Note 2)

Notes:

1. For the noted transients, the 60-year projected cycles are a summation of the normal and alternate transients:
    a. Transient 3 (Startup): Normal Startup 3-A and Alternate Startup 3-B.
    b. Transient 4 (Turbine Roll): Normal Turbine Roll 4-A and Alternate Turbine Roll 4-B.
    c. Transient 14 (Hot Standby): Normal Shutdown - Hot Standby 14-A and Alternate Shutdown - Hot Standby 14-B.
    d. Transient 15 (Shutdown): Normal Shutdown – Blowdown to Condenser 15-A and Alternate Shutdown – Blowdown to Condenser 15-B.
    e. For Transient 16 (Shutdown, Vessel Flooding): Normal Shutdown – Vessel Flood 16-A and Alternate Shutdown – Vessel Flood 16-B.

2. It is assumed that there are 40 internal cycles for each OBE event [4.b]. Therefore, 2 OBE events x 40 internal cycles = 80 OBE cycles are evaluated for 60 years of plant operation.

Table 3: Thermal Transient Definitions

Event Number**	Event Name	Time, seconds	FW Temp (H to B), °F	RPV Temp (D to G), °F	RPV Pressure, psig	Time Increment, seconds	FW Flow (%)
1	Bolt-up	0	70	70	0		0
		1080	100	70	0	1080	0
		2880	100	70	0	1800*	0
2	Design Hydrotest	0	100	100	0		0
		1	180	180	1250	1	0
		1801	180	180	1250	1800*	0
		1802	100	100	20	1	0
		3602	100	100	20	1800*	0
3a	Startup (CU heated after initiated)	0	70	100	20		0
		1080	100	100	20	1080	0
		17352	100	552	1051	16272	2
		19152	100	552	1051	1800*	2
3b**	Startup (CU heated before initiated)	0	70	100	20		0
		1080	100	100	20	1080	0
		2880	100	100	20	1800*	0
		13680	400	400	1051	10800	0
		13681	185	400.03	1051	1	2
		19152	185	552	1051	5471	2
		20952	185	552	1051	1800*	2
4a	Turbine Roll (CU heated after initiated)	0	100	552	1051		2
		1800	100	552	1053	1800	33
		1920	325	552	1055	120	33
		2520	325	552	1066	600	33
		4320	427.8	552	1100	1800	100
		6120	427.8	552	1100	1800*	100
4b**	Turbine Roll (CU heated before initiated)	0	185	552	1051		2
		1800	185	552	1051	1800*	2
		5940	70	552	1051	4140	33
		6060	325	552	1053	120	33
		6660	325	552	1065	600	33
		8460	427.8	552	1100	1800	100
		10260	427.8	552	1100	1800*	100

* Assumed for stress analysis
**Selected as bounding transient

Table 3: Thermal Transient Definitions (continued)

Event Number	Event Name	Time, seconds	FW Temp (H to B), °F	RPV Temp (D to G), °F	RPV Pressure, psig	Time Increment, seconds	FW Flow (%)
6**	Weekly Reduction, 50% Power	0	427.8	552	1100		100
		1800	427.8	552	1100	1800*	100
		1950	360	552	1063	150	50
		3750	360	552	1063	1800*	50
		3900	427.8	552	1100	150	100
		5700	427.8	552	1100	1800*	100
7	Rod Pattern Change	0	427.8	552	1100		100
		1800	427.8	552	1100	1800*	100
		2700	394	552	1078	900	75
		4500	394	552	1078	1800*	75
		5400	427.8	552	1100	900	100
		7200	427.8	552	1100	1800*	100
8**	Turbine Trip	0	427.8	552	1100		100
		1800	427.8	552	1100	1800*	100
		1890	90	552	1100	90	100
		2490	90	552	1100	600	100
		2610	325	552	1100	120	100
		3210	325	552	1100	600	100
		5010	427.8	552	1100	1800	100
		6810	427.8	552	1100	1800*	100
9	Partial FWH Bypass	0	427.8	552	1100		100
		1800	427.8	552	1100	1800*	100
		1890	265	552	1100	90	100
		3690	265	552	1100	1800*	100
		3870	427.8	552	1100	180	100
		5670	427.8	552	1100	1800*	100

* Assumed for stress analysis
**Selected as bounding transient

Table 3: Thermal Transient Definitions (continued)

Event Number	Event Name	Time, seconds	FW Temp (H to B), °F	RPV Temp (D to G), °F	RPV Pressure, psig	Time Increment, seconds	FW Flow (%)
10**	Turbine Generator Trip	0	427.8	552	1100		100
		1800	427.8	552	1100	1800*	110
		1810	396	565	1175	10	110
		1815	384	565	1175	5	110
		1830	347	538	991	15	110
		1860	275	537	987	30	110
		2760	185	512	871	900	2
		8583	185	350	120	5823	2
		12183	185	450	585	3600	2
		15753	185	549	1035	3570	33
		15855	255	552	1050	102	33
		15873	325	552	1050	18	33
		16473	325	552	1053	600	33
		18273	427.8	552	1100	1800	100
		20073	427.8	552	1100	1800*	100
11	SCRAM All Others	0	427.8	552	1100		100
		1800	427.8	552	1100	1800*	110
		1815	384	538	991	15	110
		1860	275	539	985	45	110
		2760	185	564	869	900	2
		8568	185	350	120	5808	2
		12183	185	450	585	3615	2
		15753	185	549	1035	3570	33
		15855	255	552	1050	102	33
		15873	325	552	1050	18	33
		16473	325	552	1053	600	33
		18273	427.8	552	1100	1800	100
		20073	427.8	552	1100	1800*	100
13	Reduction to 0% Power	0	400	552	1100		100
		1800	200	552	1053	1800	2
		3600	200	552	1050	1800*	2
14a	Hot Standby	0	200	552	1050		2
		1800	200	552	1050	1800*	2
		1860	100	552	1050	60	2
		3660	100	552	1050	1800*	2

* Assumed for stress analysis
**Selected as bounding transient

Table 3: Thermal Transient Definitions (continued)

Event Number	Event Name	Time, seconds	FW Temp (H to B), °F	RPV Temp (D to G), °F	RPV Pressure, psig	Time Increment, seconds	FW Flow (%)
14b	Hot Standby	0	200	552	1050		2
		1800	200	552	1050	1800*	2
		1920	435	552	1050	120	2
		2760	435	552	1050	840	0
		2761	200	552	1050	1	2
		4561	200	552	1050	1800*	2
		4681	435	552	1050	120	0
		6481	435	552	1050	1800*	0
15a	Shutdown	0	100	552	1050		2
		1800	100	552	1050	1800*	2
		12672	100	250	33	10872	2
		14472	100	250	33	1800*	2
15b**	Shutdown	0	435	552	1050		0
		1800	435	552	1050	1800*	0
		2160	425	542.0	783.3	360	0
		2161	200	542.0	782.6	1	3
		3121	200	515.3	243.7	960	3
		3241	395	512.0	188.4	120	0
		3601	385	502.0	34.0	360	0
		3602	200	502	33	1	3
		12672	200	250	33	1800*	3
16b	Vessel Flooding	0	200	250	33		3
		1800	200	250	33	1800*	3
		1801	40	250	33	1	0
		2311	40	236	33	510	0
		2312	125	236	33	1	0
		2822	125	222	33	510	0
		2823	100	222	33	1	25
		3423	100	205	33	600	25
		3424	125	205	33	1	0
		5224	125	205	33	1800*	0
17	Shutdown	0	125	205	33		0
		1800	125	205	33	1800*	0
		2700	100	179	33	900	0
		5580	100	100	33	2880	0
		7380	100	100	33	1800*	0

KLW 12/22/21

* Assumed for stress analysis, **Selected as bounding transient

Table 3: Thermal Transient Definitions (continued)

Event Number	Event Name	Time, seconds	FW Temp (H to B), °F	RPV Temp (D to G), °F	RPV Pressure, psig	Time Increment, seconds	FW Flow (%)
18	Unbolting	0	100	70	33		0
		1800	100	70	33	1800*	0
		2880	70	70	33	1080	0
		4680	70	70	33	1800*	0
20**	LOFP	0	427.8	552	1100		100
		1800	427.8	552	1100	1800*	100
		1803	424	582	1335	3	0
		1813	438	561	1125	10	0
		1815	440	561	1125	2	0
		1920	582	554	1067	105	0
		2340	525	525	833	420	0
		2700	573	567	1180	360	0
		2710	562	561	1125	10	0
		2820	561	561	1125	110	0
		3600	561	561	1125	780	0
		4020	490	490	607	420	0
		4500	573	567	1180	480	0
		4510	572	561	1125	10	0
		4620	561	561	1125	110	0
		5400	561	561	1125	780	2
		5580	530	538	961	180	2
		6000	485	485	579	420	2
		6001	100	350	120	1	33
		9601	100	518	898	3600	33
		9721	325	524	923	120	44
		10321	427.8	552	1053	600	100
		12121	427.8	552	1100	1800*	100
21**	SRV Blowdown	0	427.8	552	1100		100
		1800	427.8	552	1100	1800*	110
		1860	275	534	1093	60	110
		2400	170	375	1035	540	3
		2760	100	364	996	360	3
		11760	100	100	20	1800*	3

KLW 12/22/21

* Assumed for stress analysis
**Selected as bounding transient

Table 3: Thermal Transient Definitions (continued)

Event Number	Event Name	Time, seconds	FW Temp (H to B), °F	RPV Temp (D to G), °F	RPV Pressure, psig	Time Increment, seconds	FW Flow (%)
22**	Reactor Overpressure	0	427.8	552	1100		100
		1800	427.8	552	1100	1800*	110
		1802	422.7	594	1510	2	110
		1832	346.3	561	1175	30	110
		1860	275	561	1175	28	2
		2760	100	400	240	900	2
		2880	325	552	1050	120	33
		3480	325	552	1053	600	33
		5280	325	552	1100	1800*	100
23	Automatic Blowdown	0	427.8	552	1100		100
		1800	427.8	552	1100	1800	110
		1860	275	375	1053	60	110
		2760	100	100	709	900	3
		4560	100	100	20	1800*	3
24	Improper Start of Cold Recirculation Loop	0	394	552	1100		75
		1800	394	552	1100	1800*	75
		2700	427.8	552	1100	900	100
		4500	427.8	552	1100	1800*	100
25	Sudden Start of Pump in Cold Recirculation Loop	0	394	552	1100		75
		1800	394	552	1100	1800*	75
		2700	427.8	552	1100	900	100
		4500	427.8	552	1100	1800*	100
27	Pipe Rupture and Blowdown	0	427.8	552	1100		100
		1800	427.8	552	1100	1800*	100
		1815	259	259	1091	15	0
		3630	259	259	20	1800*	0
---	Leak Test	0	100	100	0		0
		1	100	100	400	1	0

KLW
12/22/21

* Assumed for stress analysis
**Selected as bounding transient

Table 4: Piping Load Summary [5]

Nozzle End Loads [5, Sheet 5]			
Load	H (kips)	M (inch-kips)	Radius (inch)
Deadweight	12.7	353	151
Primary Seismic	27.4	494	151
Thermal Restrained Free	58.8	1470	151

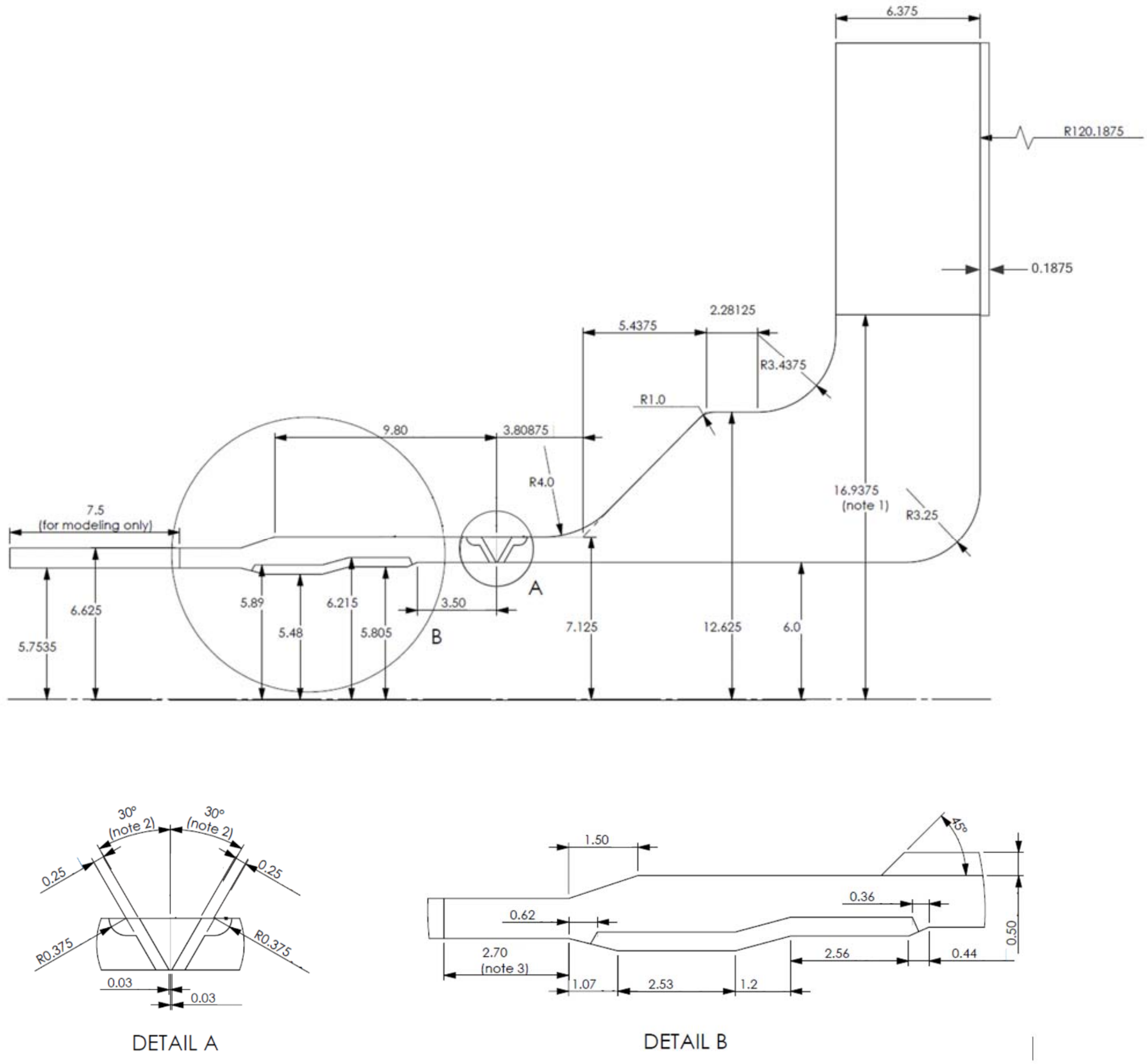

Notes: 1. This dimension is to the center of the weld.
2. "As modeled" dimension.
3. The length of straight pipe is 2.70" at the OD and 2.69" at the ID. 2.70" is modeled for both.

Figure 1. FW Nozzle as Modeled Dimensions [2]

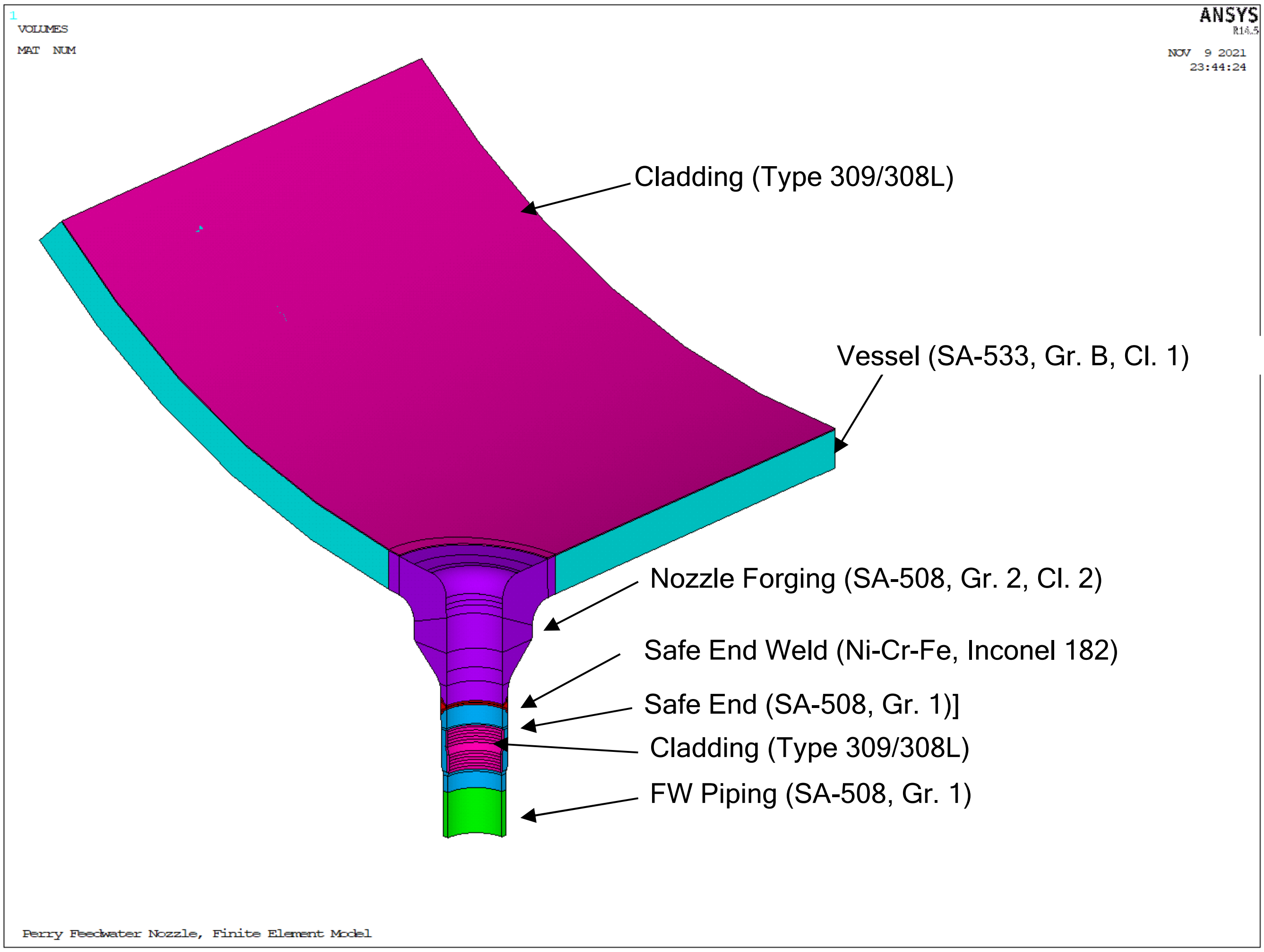

Figure 2. FW Nozzle Material Identifications

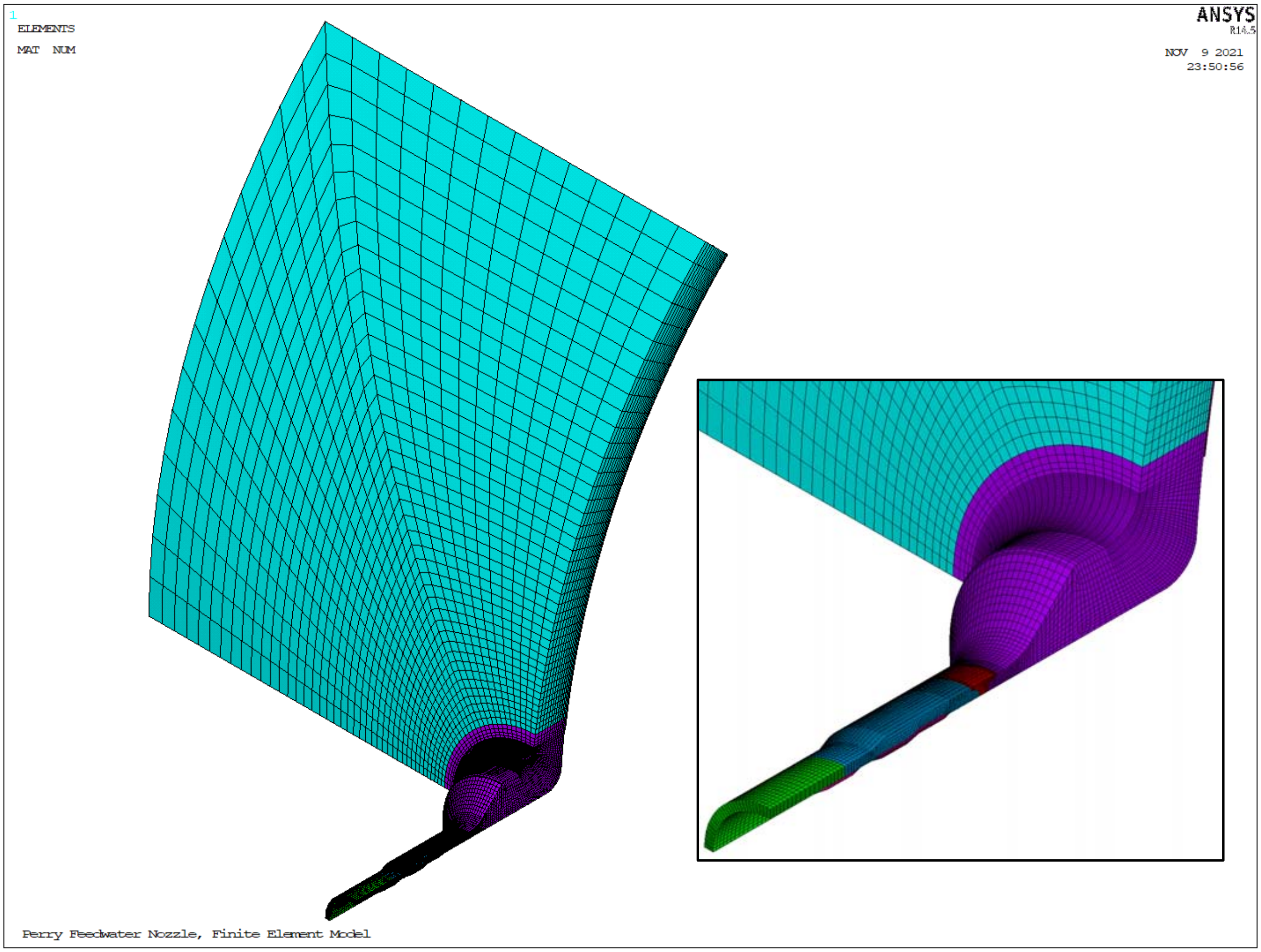

Figure 3. ANSYS Finite Element Model

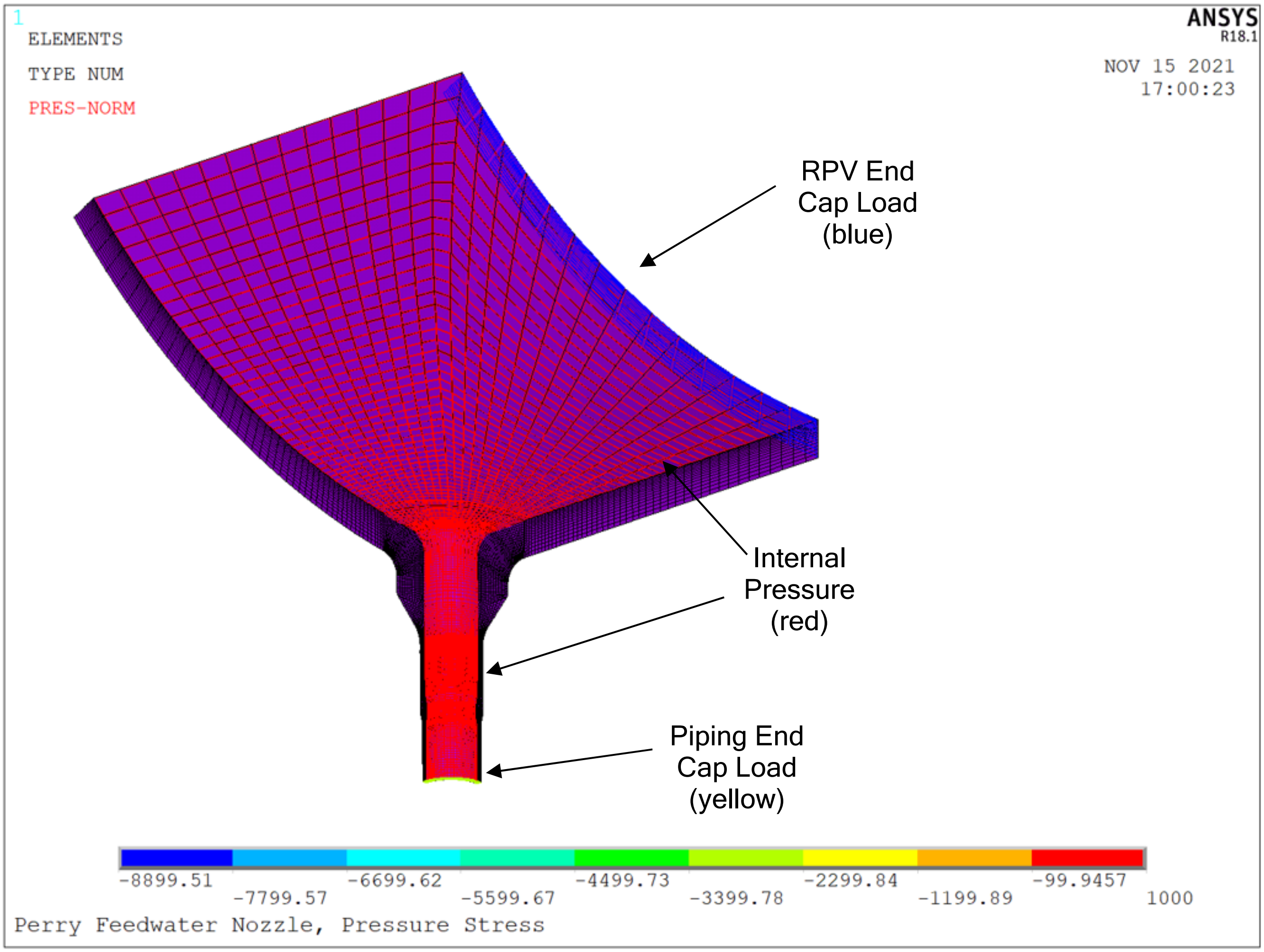

Figure 4. Pressure Load Applied to FEM (in psi)

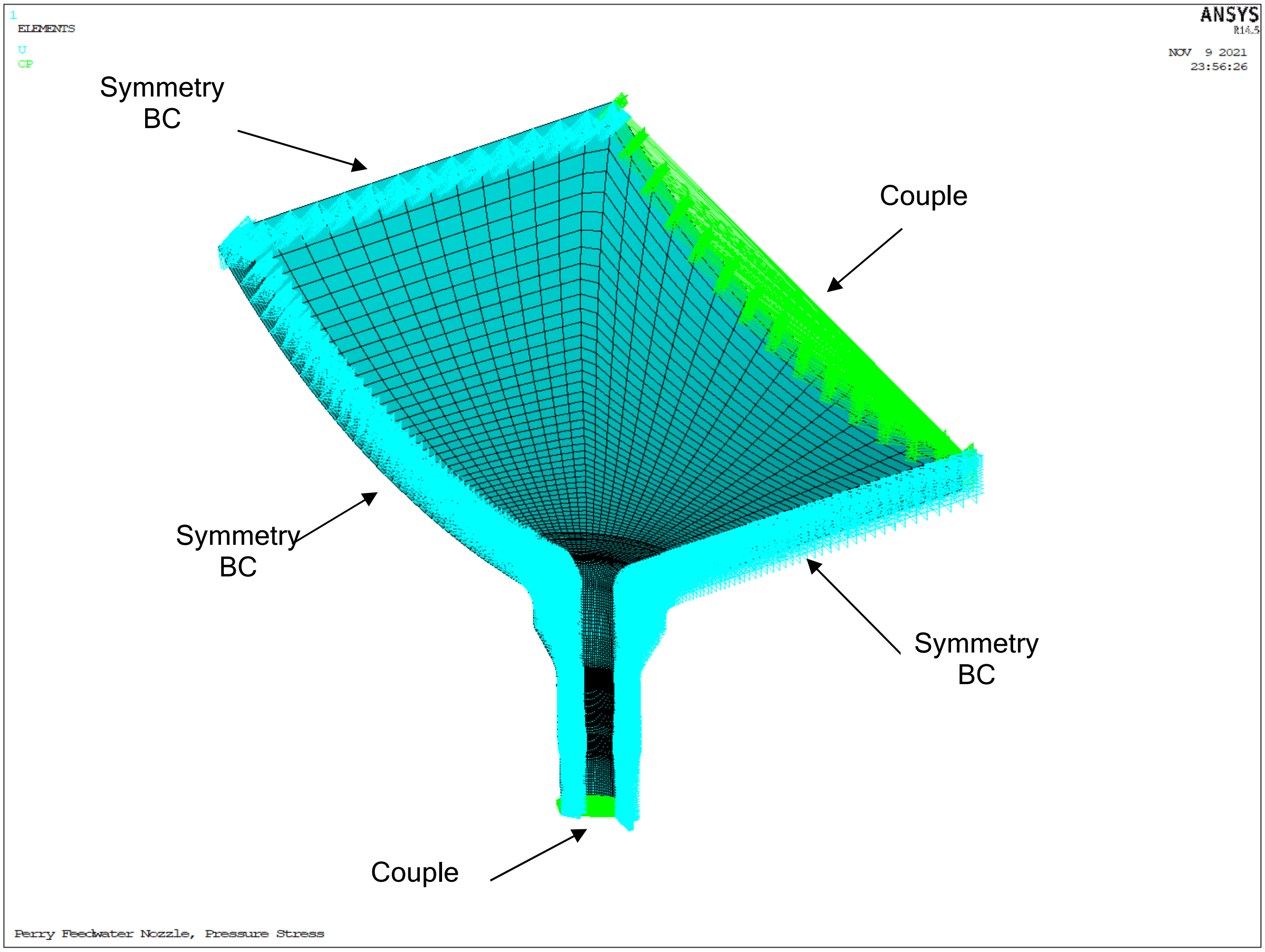

Figure 5. Mechanical Boundary Conditions (BC's)

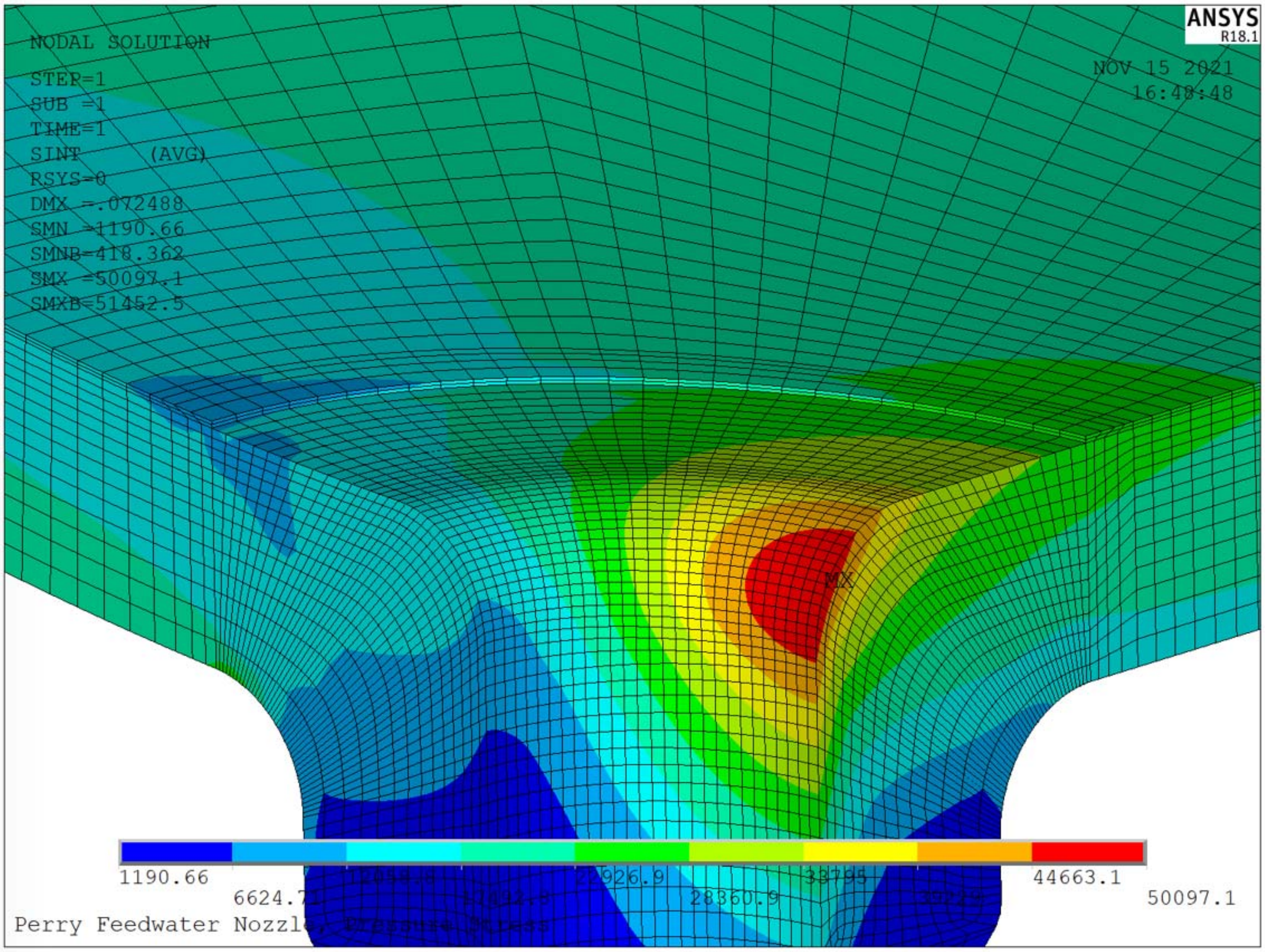

Figure 6. Original FEM Mesh Density Pressure Stress Results (in psi), Blend Radius

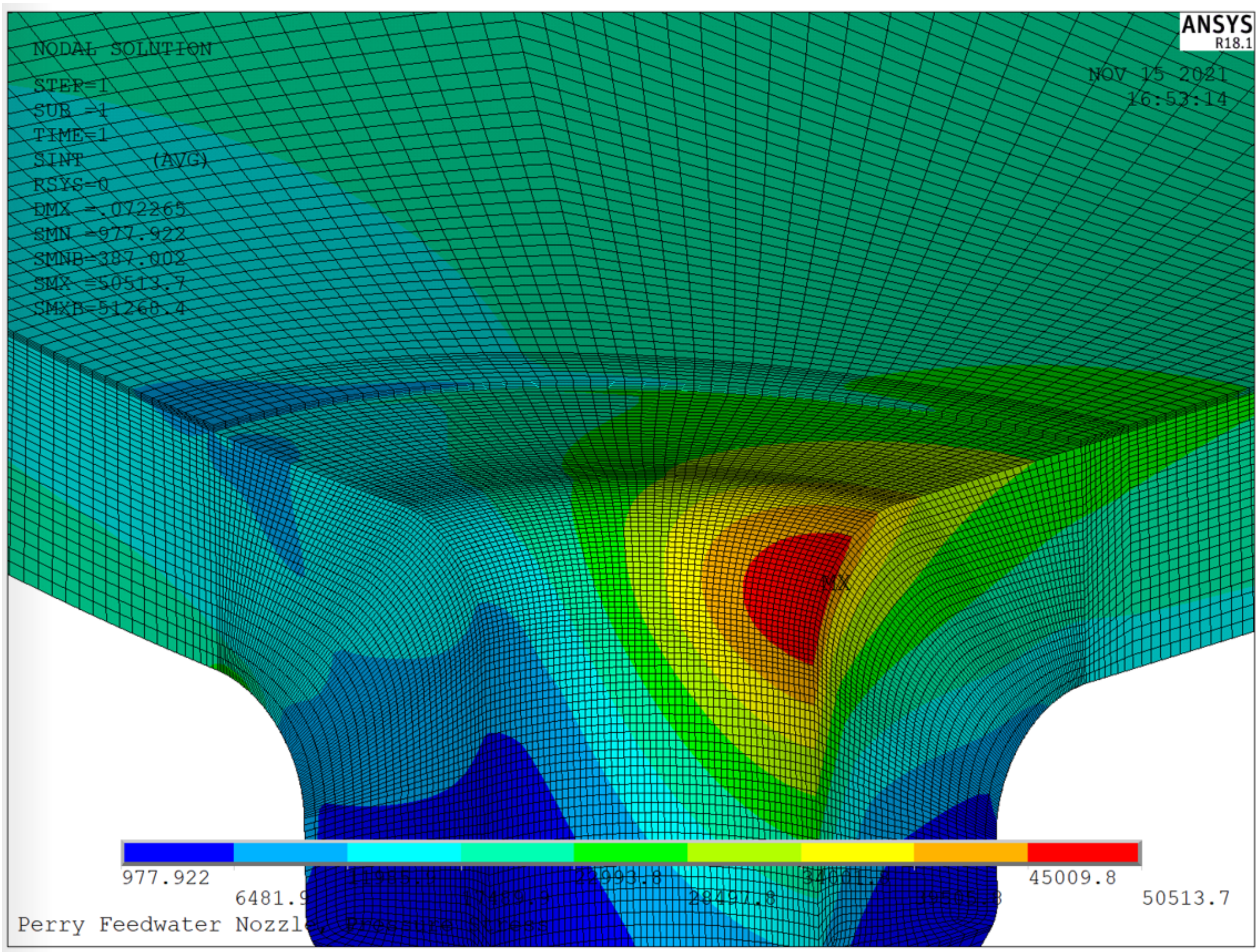

Figure 7. Refined FEM Mesh Density Pressure Stress Results (in psi), Blend Radius

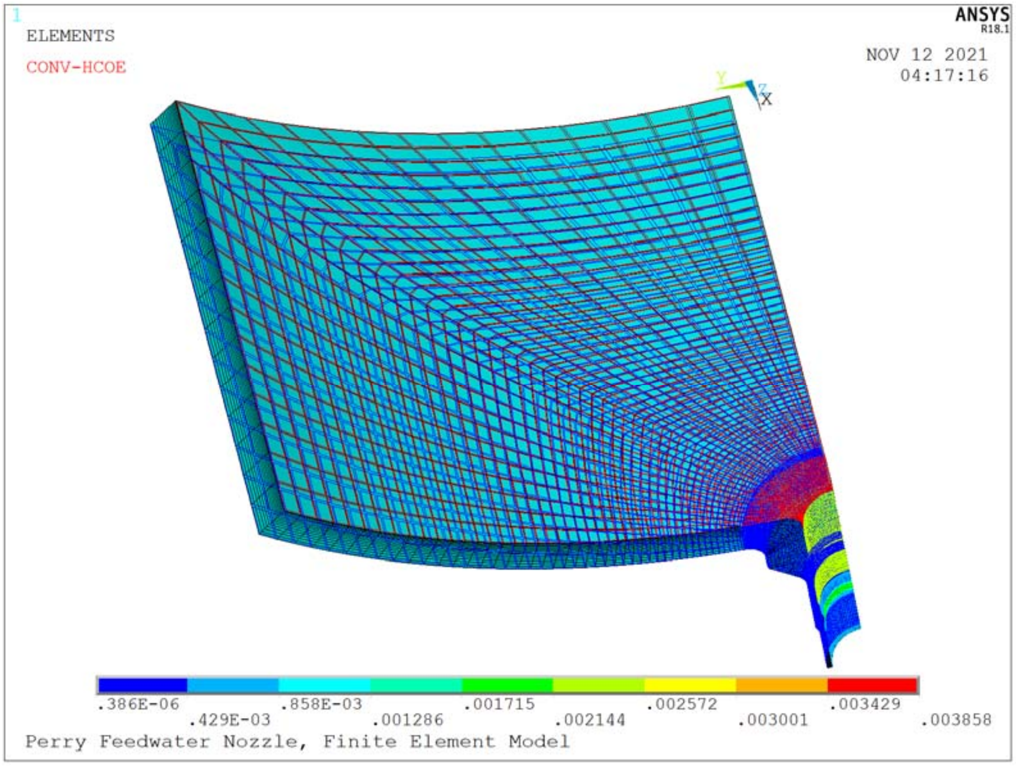

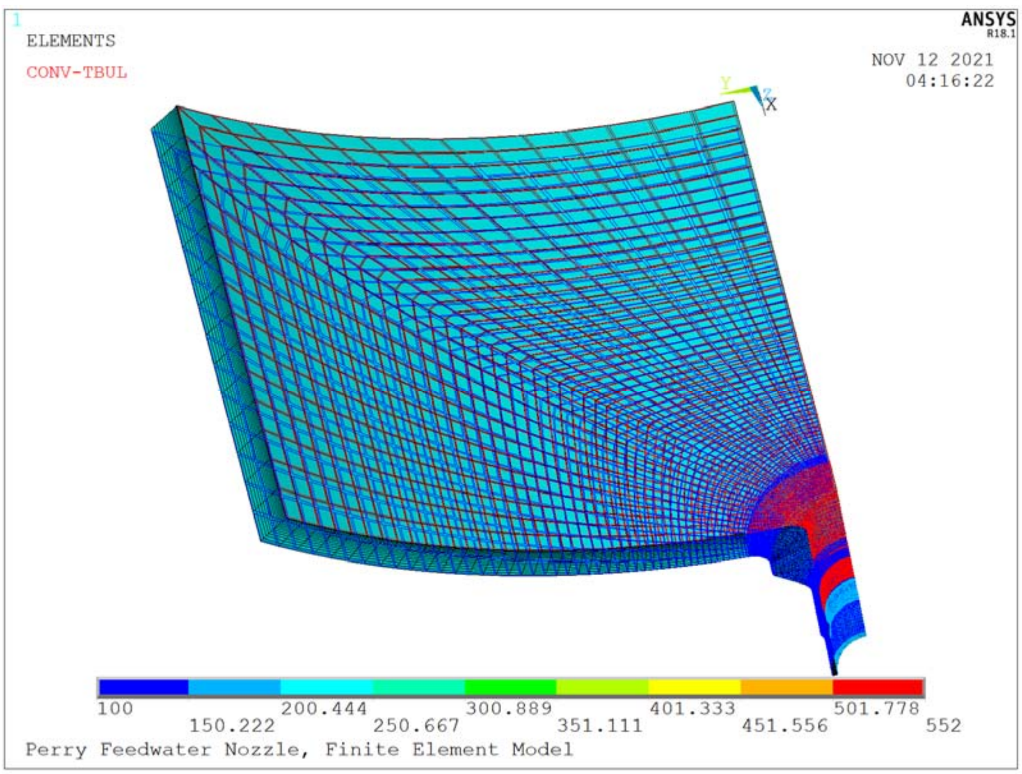

Figure 8: Typical Applied Heat Transfer Coefficient and Temperature Profile

(Top figure shows heat transfer coefficient in BTU/(sec-in^2-°F), lower figure shows applied temperature in °F.)

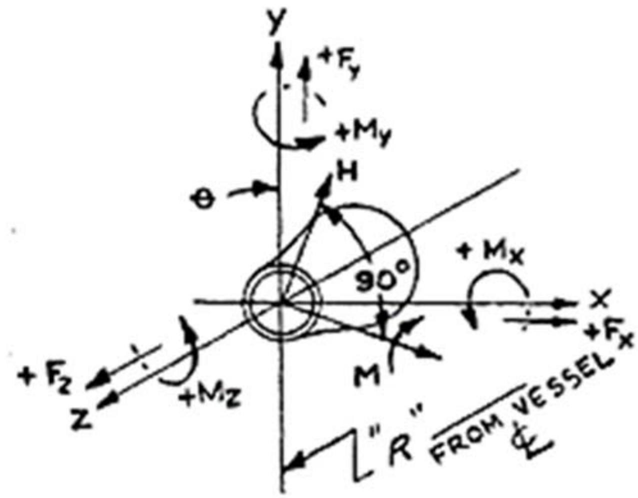

Figure 9: Piping Load Orientation

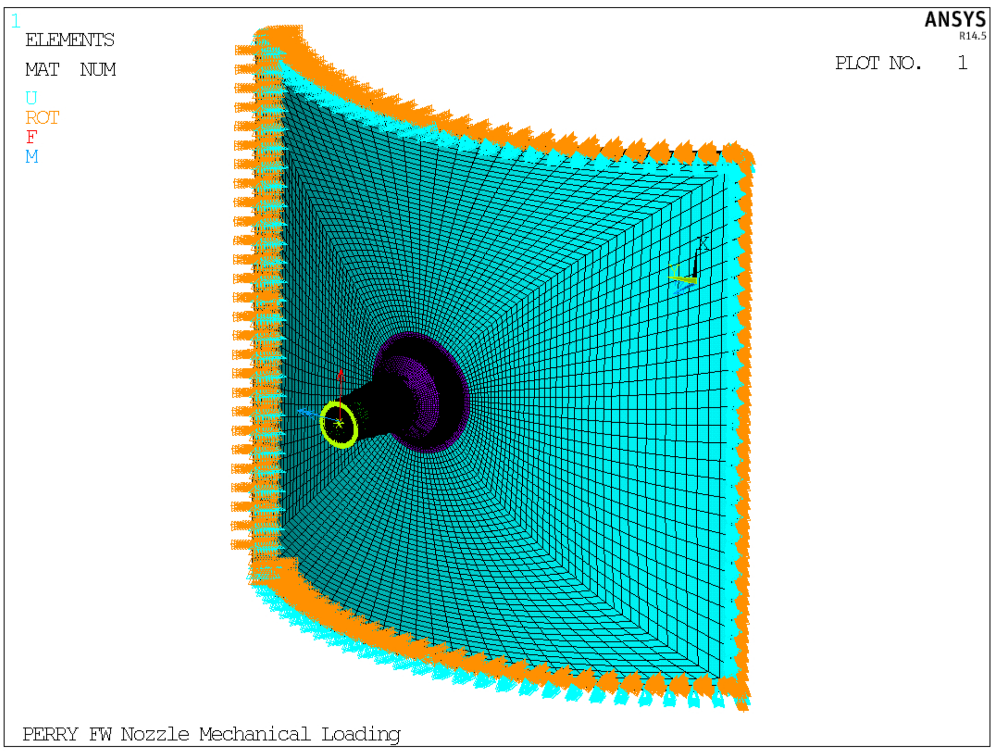

Figure 10: Piping Load Application and Boundary Conditions

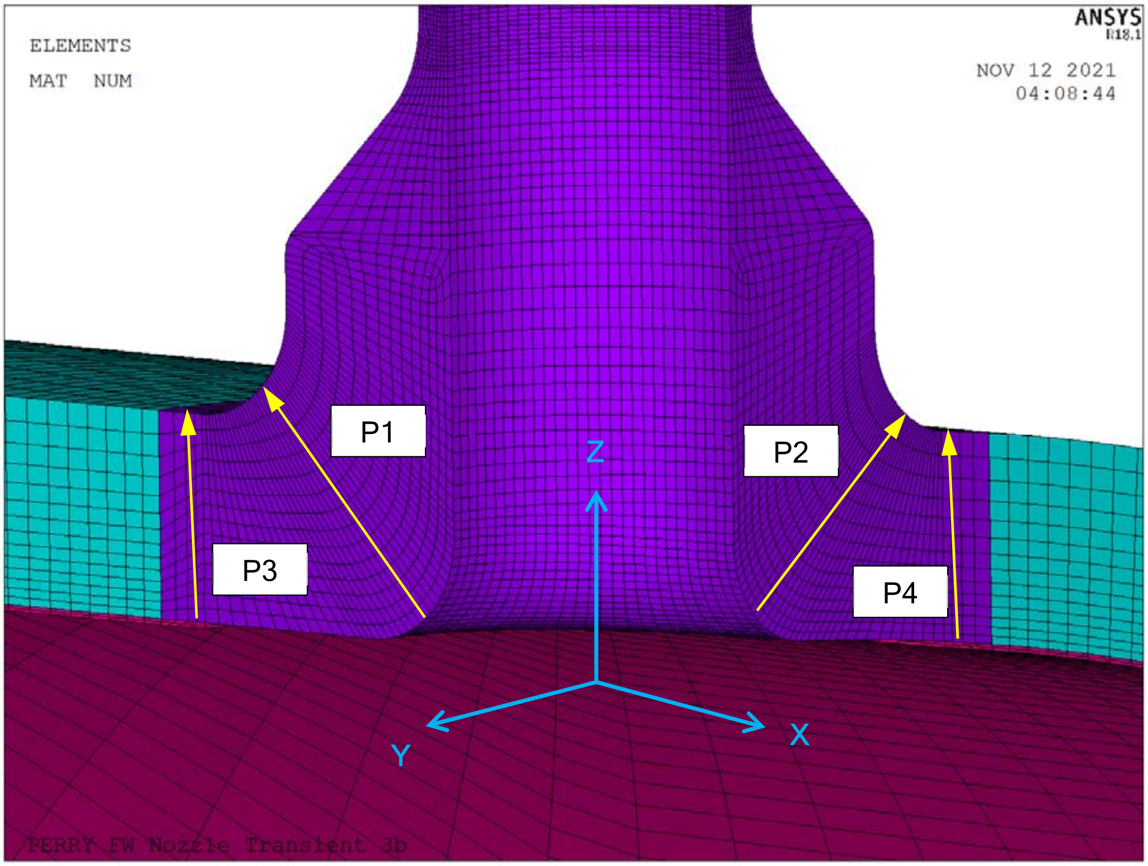

Figure 11: Stress Paths

APPENDIX A

COMPUTER FILES

LOADS CALCULATION

Filename	Description
21001178.301-HTCs.xlsm	Applied fluid temperature and heat transfer coefficients calculation in spreadsheet
21001178.301-Bounding_Transient Screening.xlsm	Bounding Transient screening in spreadsheet

FEM AND STRESS ANALYSIS

Filename	Description
FWGEOM.INP FWGEOM-2.INP	FW Nozzle finite element model
FWGEOM-Refined.INP FWGEOM-2-Refined.INP	FW Nozzle finite element model using refined mesh
Pressure.INP	FW Nozzle model under internal pressure
Pressure-Refined.INP	FW Nozzle model under internal pressure using refined mesh
FWnoz_Mechanical.INP	FW Nozzle model under mechanical piping load
FWnoz_T#.INP	APDL input file to perform thermal transient analysis
FWnoz_T#_mntr.INP	APDL input file to define load steps for thermal stress analysis
FWnoz_S#.INP	APDL input file to perform thermal stress analysis
HTBC.INP	APDL input file to apply heat transfer coefficients for thermal transient analysis
BC.inp	Structural boundary condition for thermal transient analysis
GenStress.mac	Macro that generates polynomial coefficients of stress for all paths.
GetPath.mac	Macro that generates path in ANSYS APDL
GETPATH.TXT	Text File that defines stress paths
FWNOZ_#_COE _%.CSV FWNOZ_#_MAP _%.CSV	Stress outputs* # = Pressure (Unit Pressure run) = Mechanical (Nozzle Unit Piping Load) = S3a, S4b, S6, S8, S10, S15b, S20, S21, S22 (Thermal Transient run) % = (Paths) P1, P2, P3, P4

APPENDIX B

HEAT TRANSFER CALCULATION

B.0 OBJECTIVE

The objective of this appendix is to implement the methodology of Reference [3] in calculating the applied fluid temperatures and heat transfer coefficients for each region of the FEM.

B.1 Applied Fluid Temperatures

Fluid temperature boundaries are defined [3] using the lettered nodes in Figure B-1 as guidance. The following methodology is used in defining temperatures within the following regions in Figure B-1:

H-M: $T = T_{FW}$, FW fluid temperature as defined on the FW nozzle thermal cycle diagram, °F

M-A & A-B:

$$T = T_{FW} + (C5)(T_A - T_{FW}) \tag{B-1}$$

where:

T_A = RPV Region A fluid temperature from the RPV thermal cycle diagram, °F

$C5$ = 0

Therefore, for these regions, $T = T_{FW}$

B-C: This region is assumed to be insulated

Point C:

$$T = T_{FW} + (C_1')(C_2)(T_A - T_{FW}) \tag{B-2}$$

where:

C_2 = 1.0

C_1' = 0.45 for 20% - 100% FW flow and 1.0 for 0% FW flow (linearly interpolate for flows in between 0% and 20%)

Point D: $T = T_A$

C-D: For model simplicity, the temperature between point C and D is assumed to be the average of the feedwater flow and vessel temperature in Region A. For transients with less than 20% rated feedwater flow, the temperature is assumed uniform at the vessel Region A temperature. The average temperature approach is slightly conservative when compared to the specified linear temperature transition because a larger thermal gradient will be applied to both ends of the C-D region whenever the temperatures at Point C and D differ. Therefore, Table 3 applies the average temperature in this region. If the stress analyst desires, a linear transition is also acceptable.

D-G: Same as point D

N-O: T = 100°F

B.2 Heat Transfer Coefficients for Forced and Natural Convection

Heat transfer coefficients (HTCs) are defined for regions of the model based on the thermal boundaries identified in Figure B-1. HTCs for forced flow conditions are calculated with power uprate modifications applied as appropriate. The HTCs are calculated for a range of temperatures and flow rates. Table B-3 gives the results for varying temperatures and flow rates. Maximum HTCs for each region are printed in **bold**. Bounding natural convection heat transfer coefficients are also presented.

The following methodology is used when defining the HTCs for each of the FW nozzle's regions:

<u>Forced Convection:</u>

H-I: h values based on cross-sectional properties and curve values, which are a function of temperature:

$$h = \frac{f(T)}{D\left(A/_{DF}\right)^{0.8}} \tag{B-3}$$

where:

$f(T)$ = Temperature dependent factor
D = Hydraulic Diameter, ft
A = Cross-sectional flow area, ft^2
F = Volumetric flow rate, gpm

The HTC at 100% flow is given as $h/(\%flow/100)^{0.8}$ for various temperatures. Therefore, h values at other flow rates can be calculated as:

$$h = (\%flow/100)^{0.8}\,[h/(\%flow/100)^{0.8}] \tag{B-4}$$

These h values are corrected for surface roughness of the pipe according to the following formula:

$$h' = h\left(\frac{f_{rough}}{f_{smooth}}\right) \tag{B-5}$$

The ratio (f_{rough}/f_{smooth}) ranges from 1.1 to 1.3 depending on temperature and flow rate. The computed h' values conservatively have a roughness factor of 1.3 applied to all flows at all temperatures. After the roughness factor is applied to the original h values, h_{final} is computed as follows:

$$h_{final} = h'\left[\left(\frac{\%Flow}{100}\right)\left(\frac{6555\,gpm}{7410\,gpm}\right)\right]^{0.8} \tag{B-6}$$

I-J: It is assumed that the HTCs for this region are the average between Region H-I and Region J-K [3, Assumption 3.5].

J-K & L-M: The HTC is in the same format shown in Equation B-4. These regions were analyzed for a leakage flow of 15 gpm at 25% pressure drop (100% flow). The reduced FW flow rate is assumed to have negligible impact on the leakage flow rate [3, Assumption 3.4]. Therefore, the original heat transfer formula based on percent flow is valid for power uprate flow rates. Thus, h_{final} is computed as follows:

$$h_{final} = (\%\,flow/100)^{0.8}\,[h/(\%\,flow/100)^{0.8}] \qquad \text{(B-7)}$$

K-L: This region is defined by the same h values as Regions J-K and L-M, as modified by the following equation for the insulating effect of the primary seal:

$$h_{effective} = \frac{1}{\left(\frac{L}{K}\right)_{seal} + \left(\frac{1}{h}\right)} \qquad \text{(B-8)}$$

Where:

L = Seal thickness = 0.06 in = 0.005 ft

K = Thermal conductivity of seal = 9.5 BTU/hr-ft-°F

M-A: It is assumed that the HTCs for this region are the average between Region L-M and Region A-B [3, Assumption 3.5].

A-B & C: Power uprate flow rates are used in this computation. h' is 900 Btu/(hr-ft^2-˚F) for Region A-B and C. The maximum of h_1 and h_2 below are used to then calculate the HTC for this region.

$$h_1 = \left(\frac{Z@temp\_of\_annulus}{Z@100^o F}\right)\left(\left(\frac{\%\,Flow}{100}\right)\left(\frac{6555\,gpm}{7410\,gpm}\right)\right)^{0.8}(h') \qquad \text{(B-9)}$$

$$h_2 = 0.28 * \left(\frac{Z@temp\_of\_annulus}{Z@100^o F}\right)(h') \qquad \text{(B-10)}$$

$$Z = \frac{KP_r^{\frac{1}{3}}}{\gamma^{0.8}} \qquad \text{(B-11)}$$

Where:

K = Thermal Conductivity, Btu/hr-ft-°F

P_r = Prandtl Number

Υ = Kinematic Viscosity = Dynamic Viscosity / Density, ft^2/hr

Due to the high evaluated leakage rate, the inner annulus temperature is assumed to be equivalent to the Feedwater flow temperature [3, Assumption 3.12]).

B-C: This region is assumed to be insulated.

C-E: It is assumed that the HTCs for this region are the average between Point C and Region E-G [3, Assumption 3.6]

E-G: Similar to Region A-B, the HTCs for this region are computed from the same equations but using an h' value of 3500 Btu/hr-ft^2-˚F.

O-N: This region has a constant HTC of 0.2 BTU/hr-ft^2-°F.

<u>Natural Convection:</u>

The maximum possible natural convection coefficient is 1,000 BTU/ hr-ft^2-°F. This HTC shall be used for all FW flows at 0% of rated flow, except as noted below.

K-L: This region has HTC of 655 BTU/hr-ft^2-°F.

A-B & C: The HTCs for this region and point are computed using a constant flow rate of 20% rated flow.

B-C: This region is assumed to be insulated.

C-E: It is assumed that the HTCs for this region are the average between Point C and Region E-G [3, Assumption 3.6]

E-G: Similar to Region A-B, the HTCs for this region are computed from the same equations but using an h' value of 3500 Btu/hr-ft^2-˚F.

O-N: This region has a constant HTC of 0.2 BTU/hr-ft^2-°F.

B.3 Steam Condensation

During the loss of FW pumps transient, there are times when the flow is zero and vessel water level drops below the FW nozzle, exposing the nozzle to steam. Since the nozzle and thermal sleeve are initially below the saturation temperature, laminar film condensation heat transfer occurs on the nozzle and thermal sleeve surfaces. As condensation occurs in the annular gap between the thermal sleeve and the nozzle, the condensate will flow downward and out of the gap. Additional steam will flow into the gap to replace the condensate. Therefore, the thermal sleeve can be assumed to have no effect on the heat transfer at the nozzle surface behind the gap. The average HTC for film condensation in horizontal tubes for steam condensation (known as the Kern Correlation) is given as:

$$h = 0.612\left[\frac{g\rho_l(\rho_l - \rho_v)k_l^3 h'_{fg}}{\mu_l(T_g - T_w)D}\right]^{1/4} \quad \text{(B-12)}$$

Where:

g	=	Acceleration due to gravity, 4.17 x 10^8 ft/hr^2
ρ_l	=	Mass density of liquid at average temperature, lbm/ft^3
ρ_v	=	Mass density of vapor, lbm/ft^3
k_l	=	Conductivity of liquid at average temperature, Btu/hr-ft-°F
h'_{fg}	=	$h_{fg} + 0.68c_p(T_g - T_w)$, Btu/lbm
h_{fg}	=	Heat of condensation at vapor temperature, Btu/lbm
c_p	=	Specific heat of liquid at average temperature, Btu/lb-°F
T_g	=	Saturated vapor temperature = T_{final}, °F
T_w	=	Wall temperature = $T_{initial}$, °F
μ_l	=	Dynamic viscosity of liquid at average temperature, lbm/ft-hr
D	=	Inner diameter of horizontal pipe, ft

Table B-1 and Table B-2 list selected properties of saturated water and saturated steam. Steam properties are interpolated at T_g, and water properties are interpolated at T_f, which is taken as the average of T_g and T_w. Table B-4 shows the h value calculation for steam condensation at different surface and steam temperatures for a nozzle inner diameter of 12.00 inches. The maximum h value for steam condensation is 1024 BTU/hr-ft^2-°F. Therefore, for time steps during the zero flow conditions of Transient 20 where the FW nozzle is filled with steam, a conservative HTC of 1050 BTU/hr-ft^2-°F is applied to all interior surfaces from Points H to G.

Table B-1: Thermo-Physical Properties for Saturated Water [3]

Water Property	Value at Fluid Temperature, T									
Temperature, °F	40	50	70	100	200	300	400	500	550	600
Thermal Conductivity, k, Btu/hr-ft-°F	0.325	0.332	0.347	0.364	0.394	0.395	0.381	0.349	0.325	0.292
Specific Heat, c_p, Btu/lbm-°F	1.00	1.00	0.998	0.998	1.00	1.03	1.08	1.19	1.31	1.51
Density, ρ, lbm/ft^3	62.4	62.4	62.3	62.0	60.1	57.3	53.6	49.0	45.9	42.4
Volumetric Rate of Expansion, β, 10^{-5}	2.0	4.9	12	20	40	60	80	100	110	120
Dynamic Viscosity, μ, ft^3/ft^3-°F, 10^{-5}	104	88	65.8	45.8	20.5	12.6	9.1	7.1	6.4	5.8
Prandtl Number, Pr	11.60	9.55	6.82	4.52	1.88	1.18	0.927	0.87	0.93	1.09

Table B-2: Thermal Properties for Saturated Steam [3]

Temperature T_g, °F	Specific Volume v_g, ft^3/lbm	Density ρ_g, lbm/ft^3	Enthalpy h_{fg}, Btu/lbm
500	0.6761	1.4791	714.8
510	0.6153	1.6252	701.3
520	0.5605	1.7841	687.3
530	0.5108	1.9577	672.7
540	0.4658	2.1468	657.5
550	0.4249	2.3535	641.6
560	0.3877	2.5793	625.0
570	0.3537	2.8273	607.6
580	0.3225	3.1008	589.3
590	0.2940	3.4014	570.1

Table B-3: Forced Convection Heat Transfer Coefficients, BTU/hr-ft^2-°F [3]

Thermal Boundary	Fluid Temperature °F	% Feedwater Flow 5	25	50	75	100	110
H to I	40	192	696	1212	1676	2110	2277
	50	192	696	1212	1676	2110	2277
	100	254	921	1604	2219	2793	3014
	200	358	1299	2261	3127	3936	4248
	300	424	1536	2674	3698	4655	5024
	400	455	1648	2870	3970	4997	5393
	500	461	1672	2911	4026	5068	**5469**
	552	455	1648	2870	3970	4997	5393
I to J	40	584	2116	3684	5096	6415	6923
	50	584	2116	3684	5096	6415	6923
	100	772	2798	4871	6738	8482	9154
	200	1089	3948	6874	9508	11968	12916
	300	1288	4667	8126	11239	14148	15269
	400	1382	5007	8718	12058	15179	16381
	500	1403	5083	8850	12241	15409	**16630**
	552	1382	5007	8718	12058	15179	16381
J to K and L to M	40	976	3536	6157	8516	10720	11569
	50	976	3536	6157	8516	10720	11569
	100	1290	4674	8139	11257	14170	15293
	200	1821	6598	11487	15888	20000	21585
	300	2152	7798	13578	18780	23640	25513
	400	2308	8366	14565	20146	25360	27369
	500	2344	8494	14789	20456	25750	**27790**
	552	2308	8366	14565	20146	25360	27369
K to L	40	645	1236	1452	1553	1614	1632
	50	645	1236	1452	1553	1614	1632
	100	768	1351	1540	1626	1675	1690
	200	930	1475	1630	1697	1735	1746
	300	1009	1528	1667	1725	1759	1768
	400	1042	1548	1681	1736	1768	1777
	500	1049	1553	1684	1739	1769	**1778**
	552	1042	1548	1681	1736	1768	1777
M to A	40	576	1862	3242	4484	5645	6092
	50	576	1862	3242	4484	5645	6092
	100	771	2472	4304	5953	7493	8087
	200	1099	3501	6095	8430	10612	11452
	300	1306	4145	7217	9983	12566	13562
	400	1406	4452	7752	10722	13497	14566
	500	1429	4521	7872	10888	13706	**14792**
	552	1404	4450	7748	10717	13490	14559

Table B-3: Forced Convection Heat Transfer Coefficients, BTU/hr-ft2-°F [3] (continued)

Thermal Boundary	Fluid Temperature °F	% Feedwater Flow 5	25	50	75	100	110
A to B and Point C	40	176	188	327	452	569	614
	50	176	188	327	452	569	614
	100	252	269	469	648	816	881
	200	378	404	703	972	1223	1320
	300	461	492	857	1185	1492	1610
	400	504	539	938	1297	1633	1762
	500	513	548	955	1321	1662	1794
	552	500	535	931	1287	1620	1749
	600	485	518	902	1247	1570	1695
B to C	All	Insulated					
C to E	50	430	459	799	1105	1392	1502
	100	616	658	1146	1584	1994	2152
	200	924	986	1717	2375	2990	3227
	300	1126	1203	2095	2897	3647	3936
	400	1233	1317	2293	3171	3992	4308
	500	1255	1341	2334	3228	4064	4386
	600	1193	1266	2204	3049	3838	4142
E to G	50	684	730	1271	1759	2214	2389
	100	980	1047	1822	2521	3173	3424
	200	1469	1569	2732	3779	4757	5134
	300	1792	1914	3332	4609	5802	6261
	400	1961	2095	3648	5045	6351	6854
	500	1997	2133	3713	5136	6465	6977
	600	1886	2014	3507	4851	6106	6590
O to N	All	0.2	0.2	0.2	0.2	0.2	0.2

Table B-4: Steam Condensation Heat Transfer Coefficients, BTU/hr-ft^2-°F [3]

$h = 0.612 * \{\rho_l(\rho_l - \rho_v) g k_l^3 h'_{fg} / [\mu d(T_g - T_w)]\}^{1/4}$ [29]   g 4.17E+08

$h'_{fg} = h_{fg} + 0.68 c_p (T_g - T_w)$, [29]

D (in)= 12.00

T_g	ρ_v, lbm/ft^3	h_{fg}, Btu/lbm	T_f, °F	ρ_l, lbm/ft^3	c_p, Btu/lbm-°F	μ_l, lbm/ft-hr	k_l, Btu/hr-ft-°F	T_w,°F	h'_{fg}, Btu/lbm	h, Btu/hr-ft^2-°F
561	2.6041	623.3	494.4	49.3	1.184	0.260	0.351	427.8	730.5	592
561	2.6041	623.3	525.5	47.3	1.271	0.244	0.334	490	684.6	654
561	2.6041	623.3	556.5	45.3	1.370	0.229	0.316	552	631.6	1024

Table B-5: Bounding Transients Heat Transfer at Each Time Step

Event Number	Event Name	Time, sec	FW Temp (H to B) (°F)	Average Temp (C to D) (°F)	Reactor Temp (D to G) (°F)	HI	IJ	JK	KL	LM	MA	AB	CD	DE	EG
			Tfw	Tave	Tvess	HHI	HIJ	HJK	HKL	HLM	HMA	HAB	HCD	HDE	HEG
3b	Startup (CU heated before initiated)	0.001	70	85	100	2400	7300	12100	1700	12100	6400	700	1900	2000	3200
		1080	100	100	100	1000	1000	1000	700	1000	1000	600	1300	1300	2000
		2880	100	100	100	1000	1000	1000	700	1000	1000	600	1300	1300	2000
		13080	383	383	383	1000	1000	1000	700	1000	1000	600	1300	1300	2000
		13680	400	400	400	1000	1000	1000	700	1000	1000	600	1300	1300	2000
		13680.001	185	400	400	300	700	1100	900	1100	800	400	1300	1300	2000
		14280	185	417	417	300	700	1100	900	1100	800	400	1300	1300	2000
		18552	185	535	535	300	700	1100	900	1100	800	400	1300	1300	2000
		19152	185	552	552	300	700	1100	900	1100	800	400	1300	1300	2000
		19752	185	552	552	300	700	1100	900	1100	800	400	1300	1300	2000
		20952	185	552	552	300	700	1100	900	1100	800	400	1300	1300	2000
4b	Turbine Roll (CU heated before initiated)	0.001	185	552	552	300	700	1100	900	1100	800	400	1300	1300	2000
		1800	185	552	552	300	700	1100	900	1100	800	400	1300	1300	2000
		5640	78	328	552	1000	3000	4900	1400	4900	2600	300	1500	1600	2500
		5940	70	311	552	1000	3000	5000	1400	5000	2700	300	1600	1700	2600
		6060	325	439	552	2000	5900	9900	1600	9900	5300	700	1700	1700	2600
		6360	325	439	552	2000	5900	9900	1600	9900	5300	700	1700	1700	2600
		6660	325	439	552	2000	5900	9900	1600	9900	5300	700	1700	1700	2600
		8160	411	481	552	5500	16500	27500	1800	27500	14600	1800	4400	4300	6800
		8460	427.8	490	552	5100	15300	25500	1800	25500	13600	1700	4100	4000	6300
		8760	427.8	490	552	5100	15300	25500	1800	25500	13600	1700	4100	4000	6300
		10260	427.8	490	552	5100	15300	25500	1800	25500	13600	1700	4100	4000	6300
6	Weekly Reduction, 50% Power	0.001	427.8	490	552	5100	15300	25500	1800	25500	13600	1700	4100	4000	6300
		1800	427.8	490	552	5100	15300	25500	1800	25500	13600	1700	4100	4000	6300
		1950	360	456	552	2800	8500	14200	1700	14200	7600	1000	2400	2300	3700
		2100	360	456	552	2800	8500	14200	1700	14200	7600	1000	2400	2300	3700
		3600	360	456	552	2800	8500	14200	1700	14200	7600	1000	2400	2300	3700
		3750	360	456	552	2800	8500	14200	1700	14200	7600	1000	2400	2300	3700
		3900	427.8	490	552	5100	15300	25500	1800	25500	13600	1700	4100	4000	6300
		4050	428	490	552	5100	15300	25500	1800	25500	13600	1700	4100	4000	6300
		5700	427.8	490	552	5100	15300	25500	1800	25500	13600	1700	4100	4000	6300
8	Turbine Trip	0.001	427.8	490	552	5100	15300	25500	1800	25500	13600	1700	4100	4000	6300
		1800	427.8	490	552	5100	15300	25500	1800	25500	13600	1700	4100	4000	6300
		1890	90	321	552	2700	8100	13500	1700	13500	7200	800	3800	4000	6300
		2040	90	321	552	2700	8100	13500	1700	13500	7200	800	3800	4000	6300
		2340	90	321	552	2700	8100	13500	1700	13500	7200	800	3800	4000	6300
		2490	90	321	552	2700	8100	13500	1700	13500	7200	800	3800	4000	6300
		2610	325	439	552	4800	14500	24100	1800	24100	12800	1600	4100	4000	6300
		2760	325	439	552	4800	14500	24100	1800	24100	12800	1600	4100	4000	6300
		3210	325	439	552	4800	14500	24100	1800	24100	12800	1600	4100	4000	6300
		5010	427.8	490	552	5100	15300	25500	1800	25500	13600	1700	4100	4000	6300
		6810	427.8	490	552	5100	15300	25500	1800	25500	13600	1700	4100	4000	6300
10	Turbine Generator Trip	0	427.8	490	552	5100	15300	25500	1800	25500	13600	1700	4100	4000	6300
		1800	427.8	490	552	5500	16500	27500	1800	27500	14700	1800	4400	4300	6800
		1810	396.0	481	565	5400	16400	27300	1800	27300	14600	1800	4400	4300	6800
		1815	384.0	475	565	5400	16300	27100	1800	27100	14500	1800	4400	4300	6800
		1830	347.0	443	538	5200	15800	26400	1800	26400	14100	1700	4400	4300	6900
		1860	275.0	537	537	300	800	1300	1000	1300	900	500	1300	1300	2000
		2610	200.0	516	516	300	700	1200	900	1200	800	400	1300	1300	2000
		2760	185.0	512	512	300	700	1100	900	1100	800	400	1300	1300	2000
		3060	185.0	504	504	300	700	1100	900	1100	800	400	1300	1300	2000
		8283	185.0	358	358	300	700	1100	900	1100	800	400	1200	1200	1900
		8583	185.0	350	350	300	700	1100	900	1100	800	400	1200	1200	1900
		8883	185.0	358	358	300	700	1100	900	1100	800	400	1200	1200	1900
		12183	185.0	450	450	300	700	1100	900	1100	800	400	1300	1300	2000
		15453	185.0	541	541	300	700	1100	900	1100	800	400	1300	1300	2000
		15753	185.0	549	549	300	700	1100	900	1100	800	400	1300	1300	2000
		15855	255.0	552	552	300	800	1300	900	1300	900	500	1300	1300	2000
		15873	325.0	552	552	300	800	1400	1000	1400	900	500	1300	1300	2000
		16473	325.0	552	552	300	800	1400	1000	1400	900	500	1300	1300	2000
		16773	342.1	552	552	300	900	1400	1000	1400	1000	500	1300	1300	2000
		17973	410.7	552	552	300	900	1500	1000	1500	1000	600	1300	1300	2000
		18273	427.8	552	552	1300	3700	6200	1400	6200	3400	600	1300	1300	2100
		18573	427.8	542	552	1300	3800	6300	1400	6300	3500	600	1300	1300	2100
		20073	427.8	490	552	2100	6300	10400	1600	10400	5600	700	1700	1700	2600

Table B-5: Bounding Transients at Each Time Step (continued)

Event Number	Event Name	Time, sec	FW Temp (H to B) (°F)	Average Temp (C to D) (°F)	Reactor Temp (D to G) (°F)	HI	IJ	JK	KL	LM	MA	AB	CD	DE	EG
			Tfw	Tave	Tvess	HHI	HIJ	HJK	HKL	HLM	HMA	HAB	HCD	HDE	HEG
15b	Shutdown	0.001	435	552	552	1000	1000	1000	700	1000	1000	600	1300	1300	2000
		1800	435	552	552	1000	1000	1000	700	1000	1000	600	1300	1300	2000
		2070	428	545	545	1000	1000	1000	700	1000	1000	600	1300	1300	2000
		2160	425	542	542	1000	1000	1000	700	1000	1000	600	1300	1300	2000
		2160.001	200	542	542	300	900	1400	900	1400	900	400	1300	1300	2000
		2250	200	539	539	300	900	1400	900	1400	900	400	1300	1300	2000
		3120	200	515	515	300	900	1400	900	1400	900	400	1300	1300	2000
		3240	395	512	512	1000	1000	1000	700	1000	1000	600	1300	1300	2000
		3330	392.5	509	509	1000	1000	1000	700	1000	1000	600	1300	1300	2000
		3600	385	502	502	1000	1000	1000	700	1000	1000	600	1300	1300	2000
		3600.001	200	502	502	300	900	1400	900	1400	900	400	1300	1300	2000
		3690	200	499	499	300	900	1400	900	1400	900	400	1300	1300	2000
		12672	200	250	250	300	900	1400	900	1400	900	400	1100	1100	1700
20	LOFP	0	427.8	490	552	5100	15300	25500	1800	25500	13600	1700	4100	4000	6300
		1800	427.8	490	552	5100	15300	25500	1800	25500	13600	1700	4100	4000	6300
		1803	424.0	582	582	1050	1050	1050	1050	1050	1050	1050	1050	1050	1050
		1813	438.0	561	561	1050	1050	1050	1050	1050	1050	1050	1050	1050	1050
		1815	440.0	561	561	1050	1050	1050	1050	1050	1050	1050	1050	1050	1050
		1920	582	554	554	1050	1050	1050	1050	1050	1050	1050	1050	1050	1050
		2340	525	525	525	1050	1050	1050	1050	1050	1050	1050	1050	1050	1050
		2700	573	567	567	1050	1050	1050	1050	1050	1050	1050	1050	1050	1050
		2710	562	561	561	1050	1050	1050	1050	1050	1050	1050	1050	1050	1050
		2820	561	561	561	1050	1050	1050	1050	1050	1050	1050	1050	1050	1050
		3600	561	561	561	1050	1050	1050	1050	1050	1050	1050	1050	1050	1050
		4020	490	490	490	1050	1050	1050	1050	1050	1050	1050	1050	1050	1050
		4500	573	567	567	1050	1050	1050	1050	1050	1050	1050	1050	1050	1050
		4510	572	561	561	1050	1050	1050	1050	1050	1050	1050	1050	1050	1050
		4620	561	561	561	300	900	1400	1000	1400	1000	500	1300	1300	2000
		5400	561	561	561	300	900	1400	1000	1400	1000	500	1300	1300	2000
		5580	530	538	538	300	900	1500	1000	1500	1000	600	1300	1300	2000
		6000	485	485	485	300	900	1500	1000	1500	1000	600	1300	1300	2000
		6000	100	225	350	1200	3500	5800	1500	5800	3100	400	1300	1600	2500
		6300	100	232	364	1200	3500	5800	1500	5800	3100	400	1400	1600	2600
		9300	100	302	504	1200	3500	5800	1500	5800	3100	400	1500	1700	2700
		9600	100	309	518	1200	3500	5800	1500	5800	3100	400	1600	1700	2700
		9720	325	425	524	2500	7500	12500	1700	12500	6600	800	2100	2100	3300
		10320	427.8	490	552	5100	15300	25500	1800	25500	13600	1700	4100	4000	6300
		10620	427.8	490	552	5100	15300	25500	1800	25500	13600	1700	4100	4000	6300
		12120	427.8	490	552	5100	15300	25500	1800	25500	13600	1700	4100	4000	6300
21	SRV Blowdown	0	428	490	552	5100	15300	25500	1800	25500	13600	1700	4100	4000	6300
		1710	427.8	490	552	5400	16400	27400	1800	27400	14600	1800	4400	4300	6800
		1800	428	490	552	5500	16500	27500	1800	27500	14700	1800	4400	4300	6800
		1860	275	405	534	4900	14700	24600	1800	24600	13100	1600	4400	4400	6900
		1980	251.7	399	511	300	900	1500	1000	1500	1000	500	1300	1300	2000
		2400	170.0	380	432	300	800	1300	900	1300	800	400	1300	1300	2000
		2760	100	364	364	200	600	1000	800	1000	700	300	1200	1200	1900
		2880	100	360	360	200	600	1000	800	1000	700	300	1200	1200	1900
		11760	100	100	100	200	600	1000	800	1000	700	300	700	700	1000
22	Reactor Overpressure	0	427.8	490	552	5100	15300	25500	1800	25500	13600	1700	4100	4000	6300
		1800	427.8	490	552	5500	16500	27500	1800	27500	14700	1800	4400	4300	6800
		1802	422.7	508	594	5500	16500	27500	1800	27500	14700	1800	4400	4200	6700
		1832	346.3	454	561	5200	15800	26400	1800	26400	14100	1700	4400	4300	6800
		1860	275	561	561	300	800	1300	1000	1300	900	500	1300	1300	2000
		1980	251.7	540	540	300	800	1300	900	1300	900	500	1300	1300	2000
		2640	123.3	421	421	200	600	900	800	900	600	300	1300	1300	2000
		2760	100	400	400	200	500	800	700	800	600	300	1300	1300	2000
		2880	325	439	552	2000	5900	9900	1600	9900	5300	700	1700	1700	2600
		3480	325	439	552	2000	5900	9900	1600	9900	5300	700	1700	1700	2600
		5280	325	439	552	4800	14500	24100	1800	24100	12800	1600	4100	4000	6300

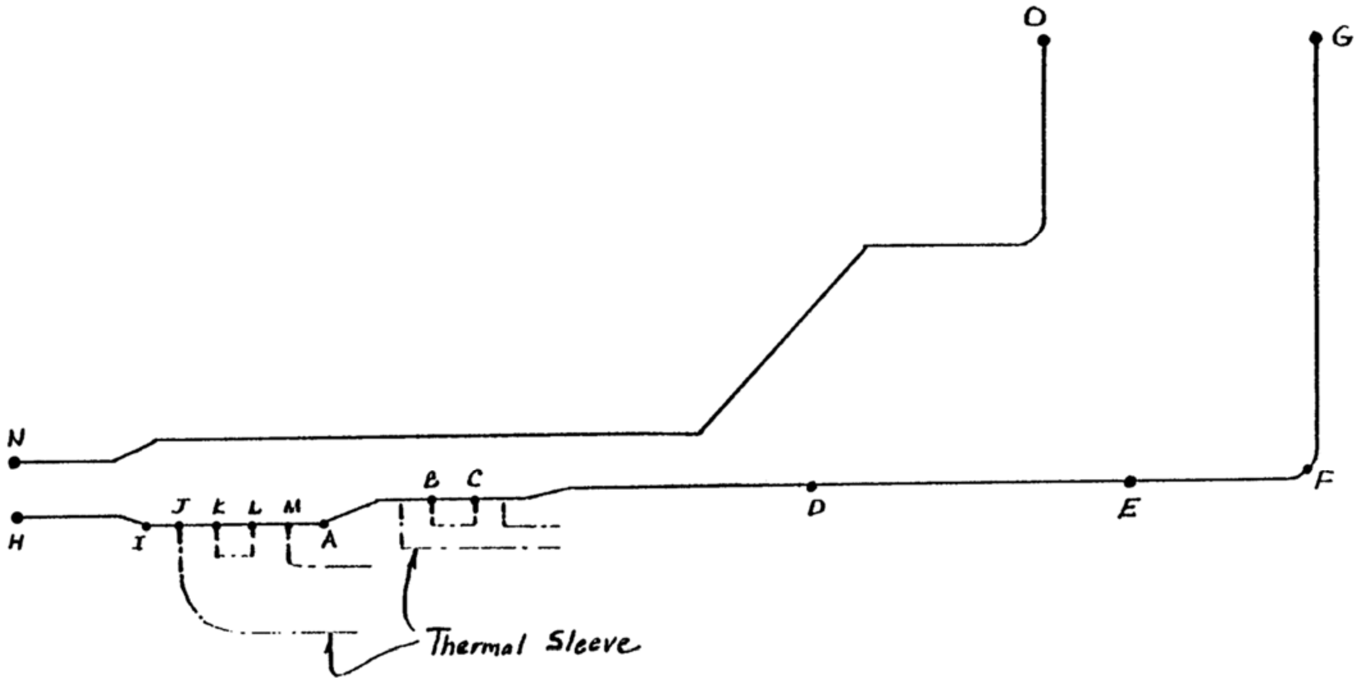

Figure B-1: FW Nozzle Thermal Boundaries [3]

Attachment 2
10 CFR 50.55a Request IR-063

Probabilistic Fracture Mechanics Evaluation for Perry Feedwater Nozzle

(30 pages follow)

File No.: 2001178.302
Project No.: 2001178
Quality Program Type: ☒ Nuclear ☐ Commercial

CALCULATION PACKAGE

PROJECT NAME:
Perry Feedwater Nozzle PFM Evaluation and Inspection Relief Request

CONTRACT NO.:
48309846

CLIENT:
Energy Harbor

PLANT:
Perry Nuclear Power Plant

CALCULATION TITLE:
Probabilistic Fracture Mechanics Evaluation for Perry Feedwater Nozzle

Document Revision	Affected Pages	Revision Description	Project Manager Approval Signature & Date	Preparer(s) & Checker(s) Signatures & Date
0	1 - 24 A-1 - A-4 B-1 - B-2	Reissue with typographical changes in red on page 11 by Kevin Wong (KLW) 12/22/21	Kevin Wong Kevin Wong 12/17/21	Kevin Wong Kevin Wong 12/17/21 GDominguez Garivalde Dominguez 12/17/21
.				

Table of Contents

List of Tables

List of Figures

1.0 INTRODUCTION

ASME Code Case N-702 [1] allows for the reduction of in-service inspection population from 100% to 25% of nozzle blend radii and nozzle-to-shell welds every 10 years for boiling water reactor (BWR) reactor pressure vessel (RPV) nozzles. Feedwater nozzles were excluded from the scope of ASME Code Case N-702 due to the cracking issues that occurred in BWR feedwater nozzle inner radii during the 1970s.

Feedwater nozzle cracking issues in BWRs were addressed by various items in NUREG-0619 [2]. Since implementation of these items the BWR fleet has operated many years and demonstrated that the cracking issues have been managed effectively. Therefore, there is now a potential to seek relief for the feedwater nozzle exam coverage. BWRVIP-108-A [3] is the technical basis for ASME Code Case N-702 for the reduction of inspection requirements for the boiling water reactor nozzle-to-vessel shell welds and nozzle inner radius. That work was supplemented by probabilistic fracture mechanics (PFM) evaluation for the BWR nozzle-to-vessel shell welds and nozzle blend radii (BWRVIP-241-A) [4]. Hence, the evaluation for the Perry Nuclear Power Plant (Perry) feedwater nozzles will follow the methodology used in BWRVIP-108-A and BWRVIP- 241-A for establishing the technical basis. Additional guidance for NRC PFM submittals is provided in EPRI Letter 2019-016 [5] and proposed NRC Regulatory Guide 1.245 [6].

A relief request [7.a] for the Columbia feedwater nozzles using the BWRVIP-108-A and BWRVIP-241-A methodology was recently approved by the NRC [7.b]. The Perry feedwater nozzle evaluation follows the methodology used in the Columbia PFM evaluation and guidance from the safety evaluation report [7.b] for the Columbia relief request. Appendix A performs a supplemental deterministic fracture mechanics evaluation, following the methodology in BWRIP-108-A.

A plant specific PFM evaluation is performed to support a relief request for reduction of inspection population from 100% to 25% every 10 years for in-service inspections (ISI) of the nozzle blend radii and nozzle-to-shell welds for the Perry feedwater nozzles. The evaluation will include 25% inspection of the feedwater nozzle population for every ten years from the fourth 10-year ISI interval to 60 years of plant operation for the first three 10-year ISI intervals.

2.0 METHODOLOGY

Monte Carlo simulations are performed with the SI-proprietary software VIPERNOZ [8], which was developed for RPV nozzle weld inspections with BWRVIP-108-A [3] and is the successor to the EPRI software VIPER for RPV shell weld inspections with BWRVIP-05 [9]. BWRVIP-108-A and BWRVIP-241-A use a Monte Carlo method to determine the probability of failure. The Perry feedwater nozzle stresses are used with probabilistic distributions from BWRVIP-108-A and BWRVIP-241-A to evaluate the plant specific probabilities.

The acceptance criterion from NUREG-1806 [21] limits the difference in probability of failure per year due to the low temperature over pressure (LTOP) event to be no more than $5x10^{-6}$ per year when changing from full (100%) in-service inspection (ISI) to 25% inspection of the feedwater nozzle population every ten years. Thus, the acceptance criterion is also met if the probability of failure for 25% inspection every ten years is less than $5x10^{-6}$ per year.

This analysis evaluates 25% inspection of the feedwater nozzle population every ten years from the fourth 10-year ISI interval to 60 years of plant operation with 100% inspection of the feedwater nozzle population with nozzle-specific coverage for the first three 10-year ISI intervals. If the resulting

probability of failure (PoF) per year due to a postulated LTOP event (including 1×10^{-3} probability of LTOP event occurrence per year [3, pg. 5-13]) is less than the allowable PoF of $5\text{x}10^{-6}$ per year from NUREG-1806 [21], then there is a technical basis for inspection reduction based on BWRVIP-108-A and BWRVIP-241-A. The probability of failure for normal operation is also evaluated relative to the acceptance criterion.

2.1 Assumptions

The following PFM assumptions used in the evaluation are based on previous BWRVIP development projects:

1. Flaws are assumed to be aligned parallel with the weld direction as justified in BWRVIP-05P [9].
2. One stress corrosion crack initiation and 0.1 fabrication flaws are assumed per nozzle blend radius as justified in BWRVIP-108-A SER [3.b].
3. One stress corrosion crack initiation and 1.0 fabrication flaw are assumed per nozzle/shell weld as justified in BWRVIP-108-A [3].
4. The NRC Pressure Vessel Research Users' Facility (PVRUF) flaw size distribution is assumed to apply as justified in EPRI Report W-EPRI-180-302 [20].
5. The weld residual stress distribution at the nozzle/shell weld is assumed to be a cosine distribution through the wall thickness with 8 ksi mean amplitude and 5 ksi standard deviation from BWRVIP-108-A [3].
6. Upper shelf fracture toughness is set to 200 ksi√in with a standard deviation of 0 ksi√in for un-irradiated material consistent with BWRVIP-108-A [3].
7. Standard deviation of the mean K_{IC} is set to 15 percent of the mean value of the K_{IC} as justified in BWRVIP-108-A SER [3.b].

The following are additional assumptions associated with this calculation:

8. It is assumed that there are 40 internal cycles for each OBE event [13.b].

3.0 DESIGN INPUTS

The stress analysis performed in a separate calculation [11] as design input to the PFM evaluation is described in Section 3.1. Section 3.2 describes the design inputs modeled deterministically as constants, and Section 3.3 describes the probabilistic inputs considered to be random variables.

3.1 Stress Analysis

Coefficients of linearized stresses for unit pressure (1000 psi internal pressure), deadweight, thermal moment, seismic, and the bounding thermal transients in Table 1 were extracted from the stress analysis calculation [11] using a finite element model of the Perry feedwater nozzle. Figure 1 shows the four extracted stress paths for evaluation [11, Figure 11 and Section 6.4]:

- Stress Path 1 at the nozzle blend radius (Y-direction for hoop stress)
- Stress Path 2 at the nozzle blend radius (X-direction for hoop stress)
- Stress Path 3 at the nozzle-to-shell weld (Y-direction for hoop stress)
- Stress Path 4 at the nozzle-to-shell weld (X-direction for hoop stress)

Figure 2 and Figure 3 show the through-wall stress distributions for all stress paths for the unit pressure and thermal moment, respectively. Figure 4 shows the through-wall stress distributions for all stress paths for the three most severe thermal transients. Through-wall stress distribution data and plots for all thermal transients in the stress analysis are provided in the supporting files. The stress analysis results are used as deterministic inputs described in the next sections.

3.2 Deterministic Parameters

Details of the deterministic parameters are described in the following sections.

3.2.1 RPV Dimensions

Table 3 summarizes the relevant Perry RPV dimensions [15] for the PFM evaluation.

3.2.1 Normal Operating Conditions and LTOP event conditions.

Table 3 summarizes the normal operating conditions from the feedwater thermal cycle diagrams [17] and the LTOP event pressure and temperature, which are specified in the BWRVIP-05P Safety Evaluation Report [9.b].

The stresses due to normal operating pressure and LTOP pressure for the PFM evaluation are evaluated using unit pressure stresses from the stress analysis calculation, as described in Section 3.1. The unit pressure stresses are also scaled to the minimum and maximum pressures during each bounding transient [11, Table 3] for fatigue crack growth.

3.2.2 Transients and Projected 60-Year Cycles

The thermal transients for the Perry feedwater nozzle are obtained from the thermal cycle diagrams for the RPV and feedwater nozzle [17] with consideration for extended power uprate (EPU) [18]. The stress analysis calculation tabulated the transient definitions with temperatures and pressures [11, Table 3] and selected nine bounding transients. The bounding transient criteria are (a) transients that have a large temperature difference and (b) transients that have a drastic rate of change in temperature

[11, Section 4.2]. Table 1 summarizes the thermal transients with corresponding 60-year projected cycles [13.a, Tables 8 and 9], the bounding transients with grouped cycles for evaluation, and the following notes:

- For the following transients, the 60-year projected cycles are a summation of the normal and alternate transients:
    a. Transient 3 (Startup): Normal Startup 3-A and Alternate Startup 3-B.
    b. Transient 4 (Turbine Roll): Normal Turbine Roll 4-A and Alternate Turbine Roll 4-B.
    c. Transient 14 (Hot Standby): Normal Shutdown - Hot Standby 14-A and Alternate Shutdown - Hot Standby 14-B.
    d. Transient 15 (Shutdown): Normal Shutdown - Blowdown to Condenser 15-A and Alternate Shutdown - Blowdown to Condenser 15-B.
    e. For Transient 16 (Shutdown, Vessel Flooding): Normal Shutdown - Vessel Flood 16-A and Alternate Shutdown - Vessel Flood 16-B.

- It is assumed that there are 40 internal cycles for each OBE event [13.b]. Therefore, 2 OBE events [13.a, Table 8] x 40 internal cycles = 80 OBE cycles are evaluated for 60 years of plant operation.

The stresses due to thermal transients are from the stress analysis calculation, as described in Section 3.1.

3.2.3 Piping Loads

Stresses due to piping loads [12] have been analyzed in the previous stress analysis calculation [11, Section 6.3], as described in Section 3.1. The thermal moment stresses are scaled to the minimum and maximum temperatures during each bounding transient [11, Table 3], using the following scaling T_{factor}:

$$T_{factor} = \frac{T - 70}{T_{op} - 70} \qquad (3\text{-}1)$$

where,

T_{op} = RPV normal operating temperature (°F) = 552 °F [17.a]

T = maximum or minimum operating temperature (°F)

The PFM evaluation also conservatively included stresses due to deadweight and seismic OBE, which were excluded as negligible in the Columbia feedwater nozzle PFM evaluation [7.b, Section 3.2.4]. The stresses from the seismic piping load are conservatively evaluated at the minimum and maximum temperatures for the bounding transient 3B (Startup) and the OBE cycles in Table 1.

3.2.4 In-Service Inspection

For the first 30 years of plant operation, 100% of the feedwater nozzle population has been inspected, and the minimum feedwater nozzle inspection coverages were 100% and 82.7% for the nozzle blend radius and nozzle-to-shell weld, respectively [26].

From the fourth 10-year ISI interval onward, 25% inspection is used for 40 to 60 years of plant operation.

The probability of detection (PoD) distribution function associated with inspection method is shown in Table 4 [20] and is an independent input from the ISI inspection interval, population, and coverage above. The POD curve is consistent with the POD used in BWRVIP-108-A [3.a, Figure 2-1], which included data for both the nozzle blend radius and nozzle-to-shell weld [3.b, Section 4.2].

3.2.5 Weld Residual Stresses

Consistent with BWRVIP 108-A [3], the weld residual stresses (WRS) are assumed present in the nozzle-to-shell welds for Stress Paths 3 and 4. The WRS distribution at the nozzle/shell weld is assumed to be a cosine distribution through the wall thickness with 8 ksi mean amplitude and 5 ksi standard deviation (see Figure 5). No WRS is present in the nozzle blend radius region for Stress Paths 1 and 2.

3.3 Random Variables

Random variables used in the PFM evaluation are summarized in Table 2 with details in the following sections.

3.3.1 Materials, Material Chemistry, and Fracture Toughness

Table 2 includes the weld chemistries (%Cu and %Ni) and initial $RT_{NDT\ along}$ with the standard deviation and distributions for the nozzle forging (SA-508, Gr. 2, Cl. 2) and the nozzle-to-shell welds (SA-508, Gr. 09L, CL. 2) [19]. The mean values for initial RT_{NDT} are plant-specific [19], and the remaining values and distributions are used from BWRVIP-108-A and the associated safety evaluation report [3].

Consistent with BWRVIP-108-A, the upper shelf fracture toughness of 200 ksi√in for unirradiated materials is used. The feedwater nozzles are not in the RPV beltline region and operate at high temperatures for the upper shelf fracture toughness to be applicable.

3.3.2 Fluence

The Perry feedwater nozzle (N4) experiences fluence of less than 1.00×10^{17} n/cm^2 for 54 EFPY for 60 years of plant operation [22]. As such, a bounded fluence of 1.00×10^{17} n/cm^2 is used for the evaluation of the feedwater nozzles.

3.3.3 Stress Corrosion Cracking Initiation

The stress corrosion cracking (SCC) initiation model in the VIPERNOZ program is a power law relationship. The cast stainless steel SCC data in a BWR environment is used as specified in BWRVIP-05 [9, Section 8.2.2.2], and used in BWRVIP-108-A [3] and BWRVIP-241-A [4]. Although the Perry feedwater nozzles are not cast stainless steel, sensitivity studies in BWRVIP-108-A Safety Evaluation Report concluded that use of cast stainless steel data is conservative [3.b, Section 4.5, RAI 2-10]. This model has the form;

$$T = 84.2 \times 10^{18} \sigma^{-10.5} \tag{4-1}$$

where: T = time, hours
σ = applied stress, ksi

The residual plot shows that a lognormal distribution produces the best fit for the data. The lognormal residual plot with the linear fit of the data is shown below:

$$\Phi = 0.9248x - 0.0003 \tag{4-2}$$

where: $\Phi = (x - \sigma) / \mu$
σ = data mean
μ = data standard deviation
$x = \ln (T_{actual}/T_{predicted})$

3.3.3.1 Stress Corrosion Cracking Growth

The SCC growth model in VIPERNOZ program is a power law relationship from NUREG/CR-6923 [23]. The relationship used is:

$$\frac{da}{dt} = 6.82 \times 10^{-12} K^4 \tag{4-3}$$

where: da/dt = stress corrosion crack growth rate, in/hr
K = sustained crack tip stress intensity factor, ksi√in

The residual plot shows that a Weibull distribution produces the best fit for the data. The Weibull residual plot with the linear fit of the data is shown below:

$$Y = 0.9085x - 0.3389 \tag{4-4}$$

where: Y = ln (ln (1/ (1-F)))
F = cumulative distribution from 0 to 1
x = $\ln ((da/dt)_{actual} / (da/dt)_{predicted})$

3.3.4 Fatigue Crack Growth

Consistent with BWRVIP-108-A and BWRVIP-241-A, the fatigue crack growth data for SA-533 Grade B Class 1 and SA-508 Class 2 (carbon-molybdenum steels) in a reactor water environment are reported in Reference [24] for weld metal testing at an R-ratio (algebraic ratio of K_{min}/K_{max}, "R") of 0.2 and 0.7. To produce a fatigue crack growth law and distribution for the VIPERNOZ software, the data for R= 0.7 was fitted into the form of Paris Law. The R= 0.7 fatigue crack growth law was chosen for conservatism. The curve fit result of the mean fatigue crack growth law is presented with the Paris law shown as follows:

$$\frac{da}{dn} = 3.817 \times 10^{-9} (\Delta K)^{2.927} \tag{4-5}$$

where a = crack depth, in
n = cycles

$\Delta K = K_{max} - K_{min}$, ksi-in$^{0.5}$

A comparison to the ASME Section XI fatigue crack growth law in a reactor water environment is documented in Reference [20] and it shows a reasonable comparison where the Section XI law is more conservative on growth rate at high ΔK.

Using the rank ordered residual plot, it is shown that a Weibull distribution is representative for the data. The Weibull residual plot with the linear curve fit of the data is shown below:

$$y = 4.1500x - 0.3712 \qquad (4\text{-}6)$$

where $y = \ln(\ln(1/(1-F)))$
$x = \ln((da/dn)_{actual} / (da/dn)_{mean})$
F = cumulative probability distribution

4.0 PROBABILISTIC FRACTURE MECHANICS EVALUATION

The probabilistic fracture mechanics evaluation is performed for 25% inspection of the feedwater nozzle population every ten years from the fourth 10-year ISI interval onward for up to 60 years of plant operation, after 100% inspection was performed for the first 30 years of plant operation.

For the nozzle blend radius region, a nozzle blend radius crack model [10] is used in the probabilistic fracture mechanics evaluation. For this location and crack model, the applicable stress is the stress perpendicular to a path defined 90 degrees from the tangent drawn at the blend radius.

For the nozzle-to-shell weld, either a circumferential or an axial crack, depending on weld orientation, can initiate due to either component fabrication (i.e. considering only welding process) or stress corrosion cracking. The probability of failure for a circumferential crack is less than an axial crack due to the difference in the stress (hoop versus axial) and the influence on the crack model. However, this probabilistic fracture mechanics evaluation for the nozzle and vessel shell weld considers both circumferential and axial cracks (depending on weld orientation).

An axial elliptical crack model with a crack aspect ratio of a/l = 0.5 is used in the evaluation for the nozzle-to-shell weld. The inspection probability of detection (PoD) curve in Table 4 from Reference [20, Figure 8-10] is utilized with a ten-year inspection interval. The calculation of stress intensity factor is at the deepest point of the crack.

Crack growth calculations include stress corrosion cracking and fatigue crack growth, which includes loads due to deadweight, internal pressure, nozzle moment, seismic OBE, and thermal transients.

The approach used for this evaluation is consistent with the methodology presented in BWRVIP-05 [9.a]. A Monte Carlo simulation is performed using a variant of the VIPER program [14] and follows the flow diagram in BWRVIP-05 [9.a, Figure 8-11]. The Monte Carlo method can be used to solve probabilistic problems using deterministic computation. A mean value, standard deviation, and distribution curve as defined in the random variables summary (Table 2) define a set of possible inputs and their probabilities of occurring. Using this domain of possible inputs, a set of inputs are generated

for use in determining whether the nozzle will fail using conventional deterministic fracture mechanics methodology. The number of simulations in which the nozzle is determined to fail divided by the number of simulations run (i.e., realizations) gives the probability of failure. The failure criteria are defined as:

Rupture: $K_{applied} > K_{Ic}$, where $K_{applied}$ is the applied stress intensity factor, and K_{Ic} is the fracture toughness

Leakage: Crack depth > 80% of vessel wall thickness

The VIPER program was developed as part of the BWRVIP-05 [9.a] effort for Boiling Water Reactor (BWR) reactor pressure vessel (RPV) shell weld inspection recommendations. The software was modified into a separate version in BWRVIP-108-A [3], identified as VIPER-NOZ, for RPV nozzle weld inspections, which was used in this project. The detailed description of the methodology incorporated in the VIPER and VIPER-NOZ program is documented in BWRVIP-05 [9] and BWRVIP-108-A [3], respectively. The modified software is identified as VIPER-NOZ to distinguish from the original VIPER software and is verified on a project specific basis [8] to ensure the modifications made to the VIPER software are fully quality assured.

5.0 RESULTS AND CONCLUSIONS

Table 5 presents the results of the probabilistic fracture mechanics evaluation for normal operation and LTOP events.

For normal operation, the results for Stress Path 1 at the nozzle blend radius bounds the other stress paths. For Stress Path 1, 5 failures occurred during normal operation in 1 million simulations for 60 years of plant operation. The probably of failure (PoF) for normal operation for Stress Path 1 is calculated to be 5 failures / 1 million simulations / 60 years = 8.33×10^{-8} per year. The calculated PoF for normal operation for Stress Path 1 is less than the allowable PoF of 5×10^{-6} per year from NUREG-1806 [21]. KLW 12/22/21

For LTOP events, the results for Stress Path 1 at the nozzle blend radius bounds the other stress paths. For Stress Path 1, 52 LTOP failures occurred in 1 million simulations for 60 years of plant operation. The conditional PoF for LTOP events for Stress Path 1 is calculated to be 52 failures / 1 million simulations / 60 years = 8.67×10^{-7} per year. Accounting for an LTOP event occurrence of 1×10^{-3} per year [3, pg 5-13], the calculated PoF for LTOP events for Stress Path 1 is 8.67×10^{-10} per year, which is less than the allowable PoF of 5×10^{-6} per year from NUREG-1806 [21]. KLW 12/22/21

The PFM results are also confirmed by the deterministic fracture mechanics evaluation in Appendix A, using the methodology in BWRVIP-108-A [3.a, Section 6].

Thus, using PFM methodology in BWRVIP-108-A and BWRVIP-241-A, which is the technical basis for ASME Code Case N-702, the Perry feedwater nozzles are qualified for inspection relief from 100% to 25% of the feedwater nozzle population every 10 years from the fourth 10-year ISI interval for up to sixty years of plant operation.

6.0 REFERENCES

1. ASME Code Case N-702, "Alternative Requirements for Boiling Water Reactor (BWR) Nozzle Inner Radius and Nozzle-to-Shell Welds, Section XI, Division 1," February 20, 2004.
2. U.S. NRC Report, Revision 1: BWR Feedwater Nozzle and Control Rod Drive Return Line Nozzle Cracking: Resolution of Generic Technical Activity A-10, NUREG-0619, Nuclear Regulatory Commission (NRC), November 1980.
3. EPRI BWRVIP-108-A
    a. BWRVIP-108-A: BWR Vessel and Internals Project, Technical Basis for the Reduction of Inspection Requirements for the Boiling Water Reactor Nozzle to Vessel Shell Welds and Nozzle Blend Radii, EPRI, Palo Alto, CA 2007, CA. **EPRI PROPRIETARY**.
    b. U.S. NRC Report, "Safety Evaluation by the Office of Nuclear Reactor Regulation, BWRVIP-108, BWR Vessel and Internals Project Technical Basis for the Reduction of Inspection Requirements for the Boiling Water Reactor Nozzle-to-Vessel Shell Welds and Nozzle Inner Radii," December 19, 2007, ADAMS Accession No. ML073600374.
4. BWRVIP-241-A: BWR Vessel Internal Project, Probabilistic Fracture Mechanics Evaluation for the Boiling Water Reactor Nozzle-to-Vessel Shell Welds and Nozzle Blend Radii, EPRI, Palo Alto, CA. 1021005. **EPRI PROPRIETARY**.
5. BWRVIP Letter 2019-016, from N. Palm (EPRI) to D. Rudland and P. Raynaud (U.S. NRC), White Paper on Suggested Content for PFM Submittals to the NRC, February 27, 2019, ADAMS Accession No. ML19241A545.
6. U.S. NRC DRAFT Regulatory Guide 1.245
    a. U.S. NRC DRAFT Regulatory Guide DG-1382, Proposed New Regulatory Guide 1.245, "Preparing Probabilistic Fracture Mechanics Submittals," September 2021, ADAMS Accession No. ML21034A328.
    b. U.S. NRC DRAFT Report for Comment NUREG/CR-7278, "Technical Basis for the use of Probabilistic Fracture Mechanics for Regulatory Applications," September 2021, ADAMS Accession No. ML21257A237.
7. Columbia Feedwater Nozzle Relief Request 4ISI-09
    a. Energy Northwest Letter G02-20-048, "Columbia Generating Station, Docket No. 50-397 Fourth Ten-Year Interval Inservice Inspection (ISI) Program Relief Request 4ISI-09," April 22, 2020, ADAMS Accession Number ML20114E235.
    b. U.S. NRC Report, "Safety Evaluation by the Office of Nuclear Reactor Regulation, Relief Request 4ISI-09, Alternate Examination of Reactor Vessel Feedwater Nozzles and Nozzle-to-Shell Welds, Columbia Generating Station, Energy Northwest, Docket No. 50-397," April 14, 2021, ADAMS Accession Number ML21096A048.
8. SI Calculation 2001178.303, Revision 0, "Verification of Software VIPERNOZ Version 1.3."

9. EPRI BWRVIP-05
    a. BWRVIP Report, "BWR Reactor Pressure Vessel Shell Weld Inspection Recommendations (BWRVIP-05P)," Electric Power Research Institute TR-105697, September 1995. **EPRI PROPRIETARY.**
    b. U.S. NRC Report, "Final Safety Evaluation of the BWR Vessel Internals Project BWRVIP-05 Report," TAC No. M93925, Division of Engineering Office of Nuclear Reactor Regulation, Nuclear Regulatory Commission, July 28, 1998.
10. Delvin, S. A., Riccardella, P. C., 'Fracture mechanics analysis of JAERI model pressure vessel test,' ASME PVP Conference, Paper 78-PVP-91, 1978.
11. SI Calculation Package No. 2001178.301, Revision 0, "Feedwater Nozzle Loads, Finite Element Model, and Stress Analysis."
12. CBI Nuclear Company, Charge No. 238-D4, "Subject: 238" Dia. BWR 6 Feedwater Nozzle," Section D4, Rev. 14, SI File No. 2001178.209.
13. Projected 60-Year Cycles
    a. Structural Integrity Associates Calculation No. 2001140.301, Revision 1, "Fatigue Update for Perry Nuclear Power Plant from 10/1/2016 to 10/31/2021."
    b. Email from J. Zbiegien (Energy Harbor) to K. Wong (SI), "Subject: RE: [EXTERNAL] RE: Projected Cycles," December 3, 2021 7:44AM, SI File No. 2001178.207.
14. VIPER, Vessel Inspection Program Evaluation for Reliability, Version 1.1 (April 2007), Structural Integrity Associates.
15. Energy Harbor Drawing No. 08_0021-00000, Revision 4 (CBI Nuclear Company Drawing, Contract No. 73-C108/14, Dwg. 59, Revision 3, "N4 Nozzle Forging (Feedwater)"), SI File No. 2001178.205.
16. CBI Nuclear Company Section No. 238-D11.3, Revision 5, "Perry 1 – 238 BWR 6 Vessel Contract 73-C108, Stress Report (Code), Water Lev. Instr. Nozzle Design Report – Section D 11.3," SI File No. 2001178.212.
17. Thermal Cycle Diagrams
    a. Energy Harbor Drawing No. 08-0037-00001 (General Electric Drawing No. 762E458, Revision 7, Sheet 1, "Reactor Cycles"), SI File No. 20001178.203.
    b. Energy Harbor Drawing No. 08-0037-00002 (General Electric Drawing No. 762E458, Revision 7, Sheet 2, "Reactor Cycles"), SI File No. 2001178.203.
    c. Energy Harbor Drawing Update Notice No. 08-0596-001-001, Revision 0, "Reactor Cycles," SI File No. 2001178.203.
    d. Energy Harbor Drawing Update Notice No. 08-0596-001-003, Revision 0, "Reactor Cycles," SI File No. 2001178.203.
    e. Energy Harbor Drawing No. 306-0081-00000, Revision E, "Feedwater Temperature/Pressure Cycles," SI File No. 2001178.204.
    f. Energy Harbor Drawing No. 306-0082-00000, Revision D, "Feedwater Temperature/Pressure Cycles," SI File No. 2001178.204.
    g. Energy Harbor Engineering Change Package No. 08-0596-000, Revision 0, SI File No. 2001178.204.
    h. Energy Harbor Engineering Change Package No. 08-0596-001, Revision 0, SI File No. 2001178.204.

18. General Electric Document No. 26A5308, Revision 3, “Reactor Vessel – Power Uprate,” SI File No. 2001178.206.

19. Email from J. Zbiegien (Energy Harbor) to K. Wong (SI), “Subj: PY FW Nozzle RR Design Inputs” with attachment referencing Energy Harbor Document EA-0246, Revision 0 A-02, 11/17/21 9:21AM, SI File No. 2001178.213.

20. SI Report No. W-EPRI-180-302, Revision 0, “Evaluation of effect of inspection on the probability of failure for BWR Nozzle-to-Shell-Welds and Nozzle Blend Radii Region.”

21. Technical Basis for Revision of Pressurized Thermal Shock (PTS) Screening Limit in the PTS Rule (10 CFR 50.61), NUREG-1806, Vol. 1, August 2007.

22. Email from J. Zbiegien (Energy Harbor) to K. Wong (SI), “Subj: RE: [External] RE: PY FW Nozzle RR Design Inputs” with attachment referencing Energy Harbor Document DI-EA-0235, 11/18/21 12:40PM, SI File No. 2001178.214.

23. NUREG/CR-6923, Appendix B.8, “Expert Panel Report on Proactive Materials Degradation Assessment,” Published February 2007.

24. Bamford, W. H., “Application of corrosion fatigue crack growth rate data to integrity analyses of nuclear reactor vessels,” Journal of Engineering Materials and Technology, Vol. 101, 1979, SI File No. 1300341.213.

25. EPRI Letter 2012-138, “BWRVIP Support of ASME Code Case N-702 Inservice Inspection Relief,” August 31, 2012, SI File No. 1300341.213.

26. Email from J. Zbiegien (Energy Harbor) to K. Wong (SI), “Subj: Exam Percent Coverage,” referencing Perry ISI Final Report P1R014, 12/15/21 11:36AM, SI File No. 2001178.216.

27. pc-CRACK, Version 5.0 CS, Structural Integrity Associates, Inc., December 30, 2020.

28. API 579-1/ASME FFS-1, Fitness-For-Service, June 2016.

Table 1: Bounding Thermal Transients Cycles

Perry Feedwater Transients [11, Table 2]			Bounding Analysis		
Event	Description	60-Year Projected Cycles to 11/7/2046 [13.a, Tables 8 & 9]	Bounding Group Event	New Group ID	Grouped 60-Year Cycles
1	Boltup	37	Startup	3b	260
2	Design hydrotest	47			
3	Startup	166 + 10 (Note 1)			
4	Turbine roll	167 +1 (Note 1)	Turbine Roll	4b	168
5	Daily reduction	685	Weekly Reduction	6	1806
6	Weekly reduction	436			
7	Rod pattern change	685			
8	Turbine trip	22	Turbine Trip	8	181
9	Partial feedwater heater bypass	159			
10	Turbine generator trip	13	Turbine Generator Trip	10	100
11	Other scrams	87			
13	Reduction to 0% power	209	Shutdown	15b	931
14	Hot standby	127 + 4 (Note 1)			
15	Shutdown	165 + 4 (Note 1)			
16	Shutdown, vessel flooding	160 + 10 (Note 1)			
17	Shutdown	183			
18	Unbolt	36			
19	Refueling	33			
20	Composite Loss of Feedwater Pumps	20	LOFP	20	20
21	SRV blowdown	2	SRV Blowdown	21	2
22	Reactor Overpressure	1	Reactor Overpressure	22	8
23	Automatic Blowdown	1			
24	Improper Start of Cold Recirc Loop	1			
25	Sudden Start of Pump in Cold Recirc Loop	4			
27	Pipe Rupture	1			
-	OBE	2 x 40 (Note 2)	OBE	OBE	80

Notes:

1. For the noted transients, the 60-year projected cycles are a summation of the normal and alternate transients:
    a. Transient 3 (Startup): Normal Startup 3-A and Alternate Startup 3-B.
    b. Transient 4 (Turbine Roll): Normal Turbine Roll 4-A and Alternate Turbine Roll 4-B.
    c. Transient 14 (Hot Standby): Normal Shutdown - Hot Standby 14-A and Alternate Shutdown - Hot Standby 14-B.
    d. Transient 15 (Shutdown): Normal Shutdown – Blowdown to Condenser 15-A and Alternate Shutdown – Blowdown to Condenser 15-B.
    e. For Transient 16 (Shutdown, Vessel Flooding): Normal Shutdown – Vessel Flood 16-A and Alternate Shutdown – Vessel Flood 16-B.

2. It is assumed that there are 40 internal cycles for each OBE event [13.b]. Therefore, 2 OBE events x 40 internal cycles = 80 OBE cycles are evaluated for 60 years of plant operation.

Table 2: Random Variables Parameter Summary

Source: BWRVIP-108-A [3] unless otherwise noted.

Random Parameter		Mean	Standard Deviation	Distribution	Reference
Flaw density, nozzle/shell weld (fabrication)		1 per weld	√Mean	Poisson	[3, 3, 3]
Flaw density, nozzle and nozzle/shell weld (SCC initiation)		1 per weld	√Mean	Poisson	[3, 3, 3]
Flaw density, nozzle blend radius (fabrication)		0.1 per nozzle	√Mean	Poisson	[3, 3, 3]
Flaw size (fabrication)		n/a	n/a	PVRUF	[3]
Weld residual stress, through-wall (ksi)		8 inside surface cosine distribution	5	Normal	[3, 3, 3]
N4 nozzle to shell weld	% Cu	0.26	0.045	Normal	[3, 3, 3]
	% Ni	1.2	0.0165	Normal	[3, 3, 3]
	Initial RT_{NDT} (°F)	-20	13	Normal	[19, 3, 3]
N4 nozzle forging	% Cu	0.09189	0.04407	Normal	[3, 3, 3]
	% Ni	0.78	0.068	Normal	[3, 3, 3]
	Initial RT_{NDT} (°F)	-20	26.48	Normal	[19, 3, 3]
Fast neutron fluence (n/cm^2)		1.00×10^{17}	0.2 (20%)	n/a	[22, 3]
K_{IC} upper shelf (ksi√in)		200	0	Normal	[3, 25, 3]
SCC initiation time (hr)		$T = 84.2 \times 10^{18} (\sigma)^{-10.5}$	Residual y=0.9248x-0.0003	Lognormal	[3, 3, 3]
SCCG (in/hr)		K dependent $da/dt = 6.82 \times 10^{-12} (K)^4$ K >50 ksi√in	Residual y=0.9085x-0.3389	Weibull	[23, 3, 3]
		K independent $da/dt = 2.8 \times 10^{-6}$, K <50 ksi√in	n/a	n/a	[23]
SCC threshold (ksi√in)		10	2	Normal	[3, 3, 3]
Fatigue crack growth (FCG) (in/cycle)		$da/dn = 3.82 \times 10^{-9} (dK)^{2.927}$	Residual y=4.155x-0.3712	Weibull	[3, 3, 3]
FCG threshold (ksi√in)		0	0	Normal	[3, 3, 3]

Table 3: Deterministic Parameter Summary

Parameter	Value	Reference
Dimensions		
Vessel Thickness (excludes cladding)	6.375 inches	Nozzle Drawing [15]
Vessel Radius (to vessel surface)	120.1875 inches	
Vessel Clad Thickness	0.1875 inches	Nozzle Drawing [16]
Operating Conditions - Post-EPU [18]		
Normal Operating Temperature	552 °F	RPV Thermal Cycle Diagram [17.a]
Normal Operating Pressure	1100 psig (Note 1)	Feedwater Thermal Cycle Diagram [17.e]
LTOP Event Temperature	100 °F	BWRVIP-05 SER [9.b, Section 2.6.2.2]
LTOP Event Pressure	1200 psig	

Note:

1. The higher operating pressure of the feedwater nozzle is conservatively used compared to the lower RPV operating pressure of 1050 psig [17.a].

Table 4: Probability of Detection (PoD) Distribution [20]

Flaw Size, in.	Cumulative PoD
0.00	0.20
0.05	0.32
0.10	0.46
0.15	0.61
0.20	0.75
0.25	0.85
0.30	0.91
0.35	0.95
0.40	0.96
0.45	0.97
0.50	0.98
0.55	0.99
0.60	1.00

Table 5: Probability of Failure for 60 Years of Operation

Location	Stress Path	Probability of Failure (PoF) 60 Years of Plant Operation		Allowable PoF per year NUREG-1806 [21]
		PoF per year due to Normal Operation	PoF per year due to LTOP Event (Note 1)	
Nozzle Blend Radius	1	8.33×10^{-8}	8.67×10^{-10}	5.0×10^{-6}
	2	$< 1.67 \times 10^{-8}$ (Note 2)	$< 1.67 \times 10^{-11}$ (Note 3)	
Nozzle-to-Shell Weld	3	$< 1.67 \times 10^{-8}$ (Note 2)	$< 1.67 \times 10^{-11}$ (Note 3)	
	4	$< 1.67 \times 10^{-8}$ (Note 2)	$< 1.67 \times 10^{-11}$ (Note 3)	

Notes:

(1) The LTOP PoF accounts for a 1×10^{-3} probability of LTOP event occurrence per year [3, pg 5-13].

(2) No failures occurred during normal operation. As such, the PoF for normal operation is calculated as less than 1 failure / 1 million simulations / 60 years = 1.67×10^{-8} per year.

(3) No LTOP failures occurred. As such, the LTOP PoF is calculated as less than 1 failure / 1 million simulations / 60 years * 1×10^{-3} probability of LTOP event occurrence = 1.67×10^{-11} per year.

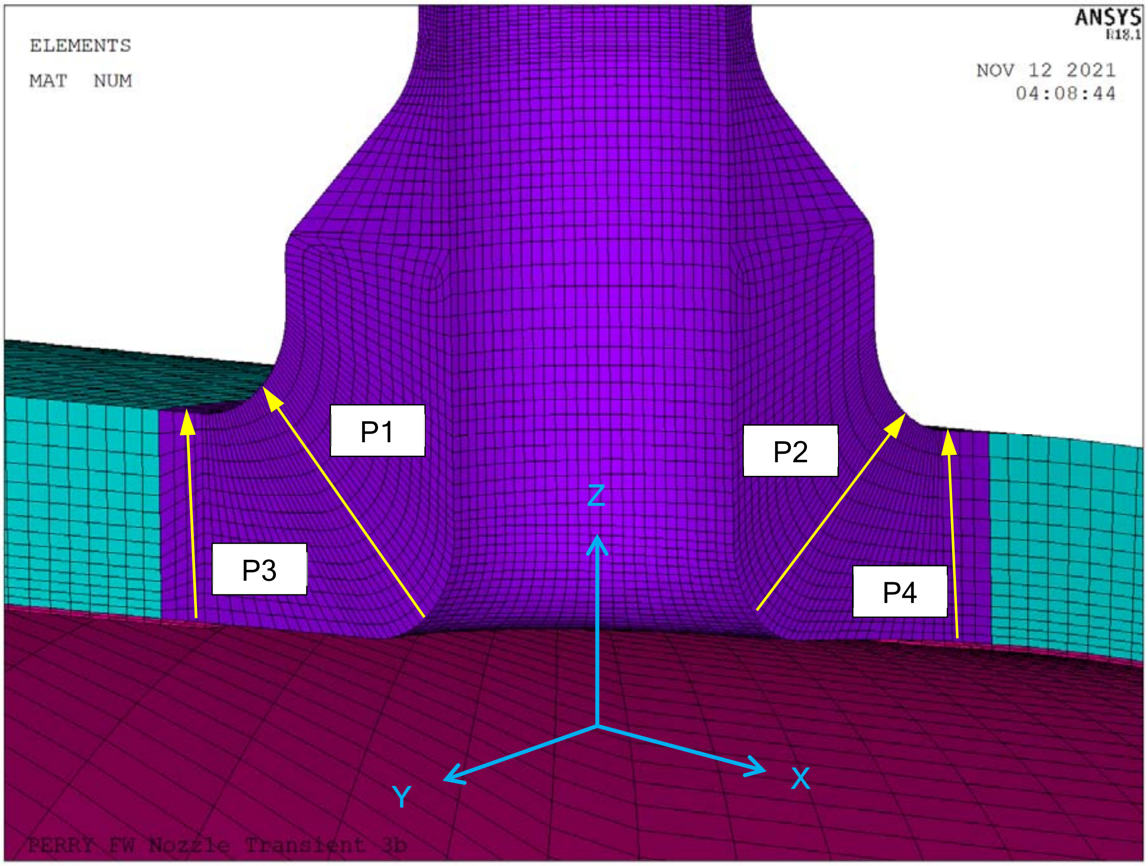

Figure 1: Stress Paths for Feedwater Nozzle

Source: Stress Analysis Calculation [11, Figure 11]

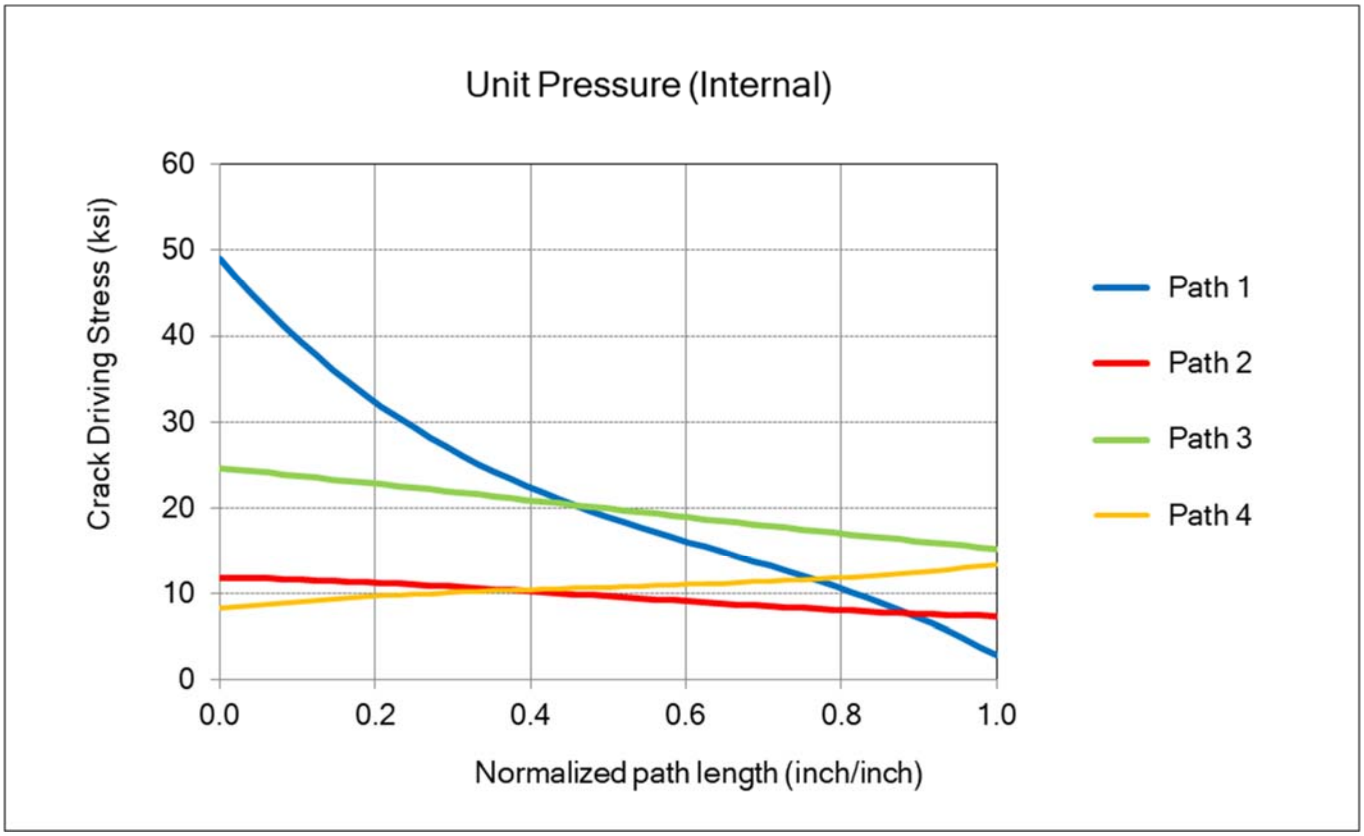

Figure 2: Through-wall Stress Distributions, Unit Pressure

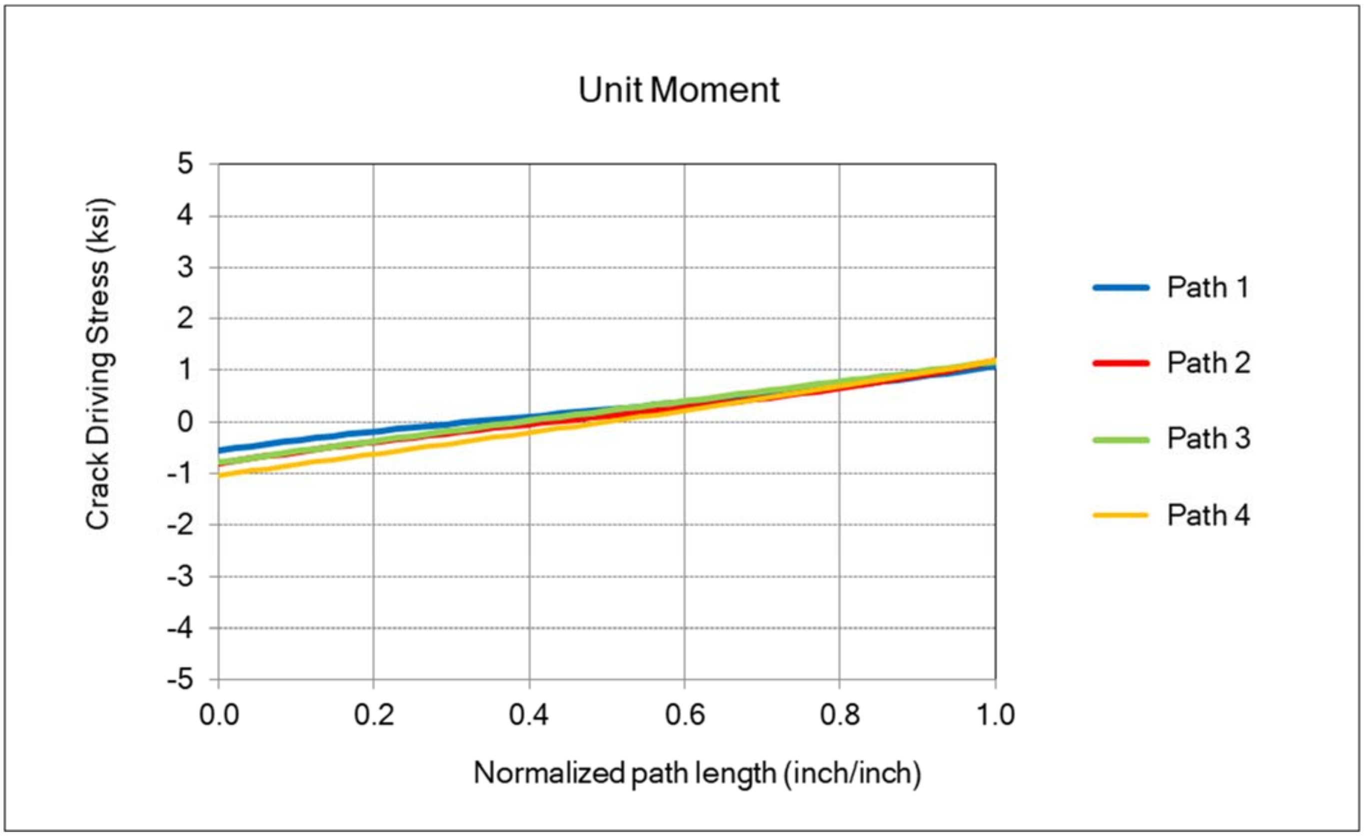

Figure 3: Through-wall Stress Distributions, Nozzle Unit Moment Load

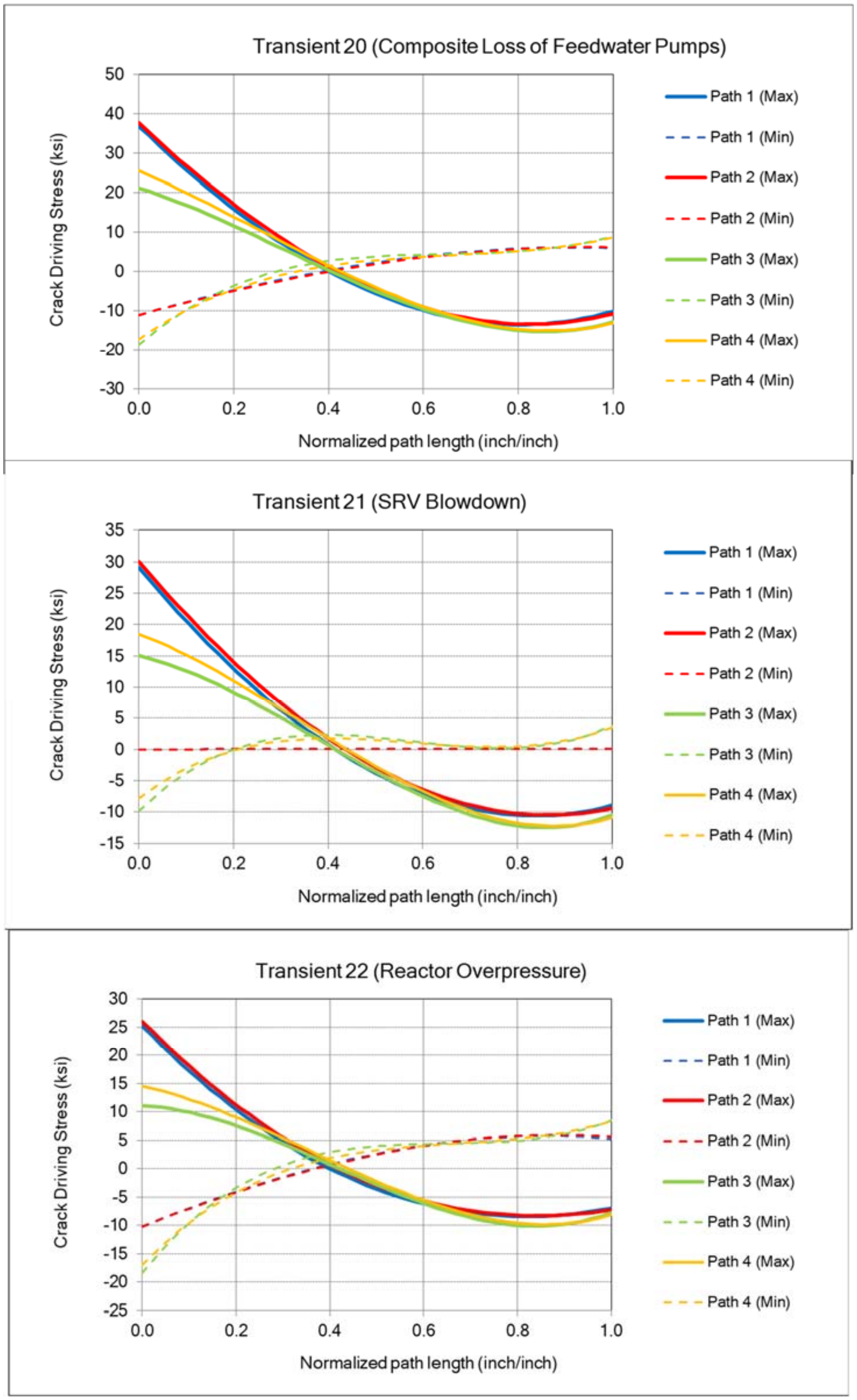

Figure 4: Through-wall Stress Distributions, Three Most Severe Thermal Transients

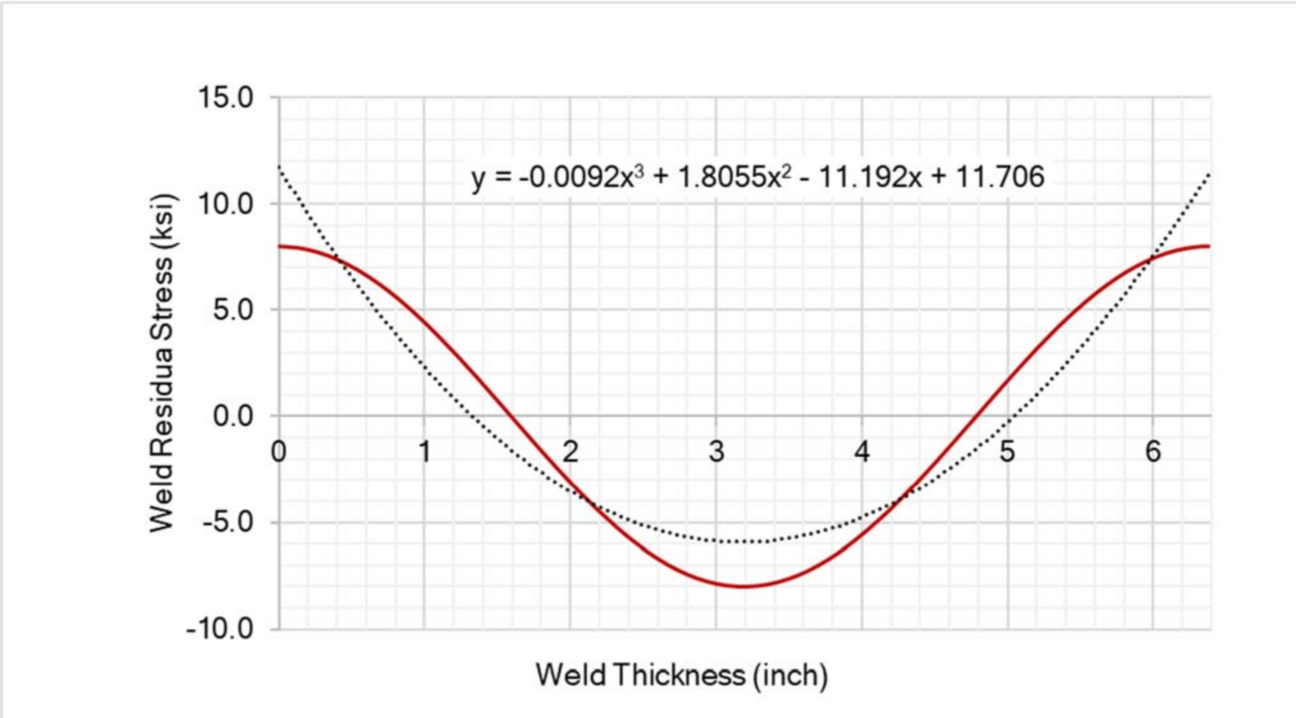

Figure 5: Weld Residual Stress Distribution for Stress Paths 3 and 4 at Nozzle-to-Shell Weld

APPENDIX A

DETERMINISTIC FRACTURE MECHANICS EVALUATION

Appendix A performs a deterministic fracture mechanics evaluation of the Perry feedwater nozzles, similar to the supplemental analysis performed for the Columbia feedwater nozzle [7.b, Section 3.2.6].

Each VIPER-NOZ simulation in the PFM evaluation consists of a series of deterministic fracture mechanics (DFM) realizations using the sampled probabilistic inputs in Table 2. A confirmatory DFM evaluation for the Perry feedwater nozzles was performed, using the methodology in BWRVIP-108-A [3.a, Section 6] and the nuclear QA fracture mechanics software, pc-CRACK 5.0 [27]. The four stress paths in the PFM evaluation were evaluated for crack growth in the DFM evaluation.

<u>Initial Flaw Size</u>

Consistent with the BWRVIP-108-A DFM evaluation, an initial flaw depth of 0.15 inch and an aspect ratio of 6:1 for the crack length to crack depth is used for both axial and circumferential cracks.

<u>Stresses</u>

The stresses for deadweight, unit pressure, unit moment, bounding thermal transients, and seismic OBE in Section 3.1 of the PFM evaluation were used for the DFM evaluation. Cyclical stresses are applied according to the grouped 60-year cycles in Table 1.

The weld residual stresses in Section 3.2.5 of the PFM evaluation were used for Stress Paths 3 and 4 at the nozzle-to-shell welds.

<u>Fracture Mechanics and Crack Growth Models</u>

The DFM evaluation used following mean values of PFM inputs in Table 2:

- Stress Corrosion Cracking: Crack growth equation and threshold value of 10 ksi√in
- Fatigue Crack Growth: Crack growth equation and threshold value of 0 ksi√in
- Material Fracture Toughness, K_{IC}, of 200 ksi√in

In the PFM analysis, the same mean parameters are used in the evaluation but with an applied standard deviations and distribution to vary for each set of realization. The fracture mechanics software pc-CRACK 5.0 includes crack models from API-579-1 [28]. For Stress Paths 1 and 2 in the nozzle blend radius, the crack model is semi-circular nozzle corner crack with a given initial depth. The cracks are modeled to propagate from the inside blend radius at the smallest distance between the inner and outer blend radius.

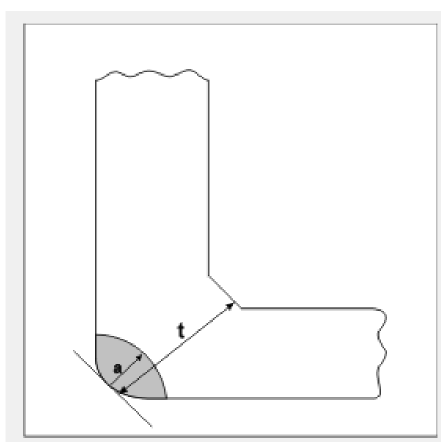

Figure A-1: Nozzle Corner Crack Model for Stress Paths 1 and 2

For the nozzle-to-shell weld, the crack-models are a semi-elliptical axial crack for Stress Path 3 and a semi-elliptical circumferential crack for Stress Path 4. They are developed from the inside surface of a cylinder with a given initial depth and length. The cracks are propagated through the cylinder wall thickness from the inside radius to outside radius in depth and length with a fixed aspect ratio.

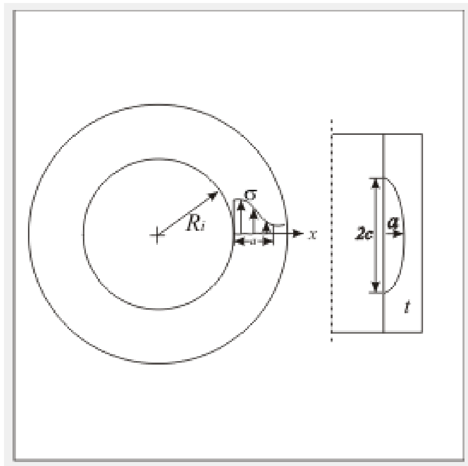

Figure A-2: Semi-Elliptical Axial Crack in a Cylinder Model for Stress Path 3

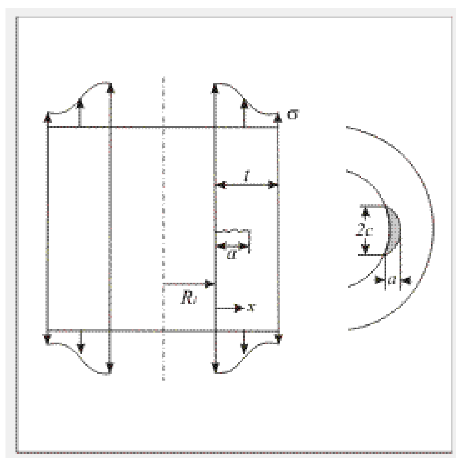

Figure A-3: Semi-Elliptical Circumferential Crack in a Cylinder Model for Stress Path 4

DFM Results

The results of the DFM evaluation after 60 years of plant operation are in terms of the final flaw depth, a_f, the final depth-to-thickness ratio, a_f/t, and the applied stress intensity factor, K_i, of the final flaw size as compared to the fracture toughness of the material, K_{IC}. For all stress paths after 60 years of crack growth, the final flaw depth is less than 10% of the thickness, and the final applied stress intensity factor is less than 50% of the material fracture toughness. Results of the DFM evaluation using average values show that fracture for all four stress paths is not expected since the crack growth is not significant if the average growth rate is used, consistent with DFM evaluations in BWRVIP-108-A [3.a, Section 6] and the Columbia supplemental analysis [7.b, Section 3.2.6].

Location	Stress Path	DFM Crack Growth 60 Years of Operation			Material Fracture Toughness K_{IC} (ksi√in)
		Final Flaw Depth		Final K_i (ksi√in)	
		a_f (inch)	a_f/t		
Nozzle Blend Radius	1	0.60	0.065	91.8	200
	2	0.16	0.018	26.0	
Nozzle-to-Shell Weld	3	0.35	0.055	46.1	
	4	0.32	0.050	43.7	

APPENDIX B

SUPPORTING FILES

Stress Analysis Supporting Files

Filename	Description
2001178.302 - Stresses.xlsx	Stress coefficients and through-wall stress plots for unit pressure, deadweight, unit moment, seismic, and thermal transients from the stress analysis calculation [11].

Probabilistic Fracture Mechanics Supporting Files

PFM / File Name	Description
Path1.INP Path1.OUT	VIPERNOZ input and output files for Path 1 at nozzle blend radius.
Path2.INP Path2.OUT	VIPERNOZ input and output files for Path 2 at nozzle blend radius.
Path3.INP Path3.OUT	VIPERNOZ input and output files for Path 3 at nozzle-to-shell weld.
Path4.INP Path4.OUT	VIPERNOZ input and output files for Path 4 at nozzle-to-shell weld.
VIPERNOZ1p3.EXE	VIPERNOZ executable program
ISPCTPOD.INP	VIPERNOZ probability of detection curve input file
FLWDSTRB.INP	VIPERNOZ flaw size distribution curve input file

Deterministic Fracture Mechanics Supporting Files

DFM / File Name	Description
Path1.INP Path1.OUT	pc-CRACK input and output files for Path 1 at nozzle blend radius.
Path2.INP Path2.OUT	pc-CRACK input and output files for Path 2 at nozzle blend radius.
Path3.INP Path3.OUT	pc-CRACK input and output files for Path 3 at nozzle-to-shell weld
Path4.INP Path4.OUT	pc-CRACK input and output files for Path 4 at nozzle-to-shell weld